MIXING PROCESSES FROM CTD PROFILES USING A LAKE-SPECIFIC EQUATION OF STATE: QUESNEL LAKE

by

CHRISTINA JAMES
B.Sc., University of British Columbia, 2001

A THESIS SUBMITTED IN PARTIAL FULFILMENT OF
THE REQUIREMENTS FOR THE DEGREE OF
MASTER OF APPLIED SCIENCE

in

THE FACULTY OF GRADUATE STUDIES

(Department of Civil Engineering;
Environmental Fluid Mechanics)

UNIVERSITY OF BRITISH COLUMBIA

November 2004

©Christina James, 2004

Abstract

Quesnel Lake, is a deep (511m maximum depth) fjord-type lake in northeast British Columbia, Canada. Mixing processes in the lake exchange deep-water with surface water and contribute to the renewal of surface-water nutrients and oxygenated deep-water. These processes are of great consequence to the lake's trophic dynamics and understanding them will enable better management of the large salmon resources in Quesnel Lake.

To better understand large-scale convective processes, a lake-specific equation of state was developed. Water samples were collected at locations around Quesnel Lake and analysed for ionic and non-ionic composition as well as other quantities that are integral to determining the lake's equation of state including pH, alkalinity and specific conductance. A relationship was developed to find lake water salinity from CTD data. Salinity was in turn related to density using a modified form of a general limnological equation of state. The equation of state developed for Quesnel Lake gives densities accurate to $\pm$ 0.0018 kg/m^3 whereas the general equation of state (based on seawater composition) is only accurate to $\pm$ 0.0158kg/m^3 for Quesnel Lake water samples.

The lake-specific equation of state was used to identify gravitational instability in density profiles estimated from CTD data. In order to compare water parcel density within a profile, the hydrostatic pressure effect must be removed. The three quantities that are used for this purpose, potential density, quasi-density and standard density, were compared. Quasi-density was found to be most appropriate for Quesnel Lake's deep water which is near the temperature of maximum density. Quesnel lake water column stability was quantified using the Brünt-Väisäla frequency calculated using quasi-density.

Contents

List of Figures

List of Tables

List of Notations

List of Symbols

A..... the coefficient of proportionality between specific conductance and salinity

B..... percentage offset of Quesnel Lake coefficient of haline contraction to coefficient of haline contraction in equation of state developed by Chen and Millero (1986)

c_i..... measured concentration of ion i

C..... conductivity

C_T^p.... conductivity measured at temperature T and pressure P

D..... standard density

f_i..... reduction coefficient of ion i

f_P.... pressure factor

f_T.... temperature factor

m.... concentration of a dissolved solid in Quesnel Lake

$\mathbf{N}$.... Brünt Väisäla frequency or stability frequency

p..... pressure

r..... conductivity ratio

R^2.... coefficient of determination

S..... salinity

S_o.... reference salinity used in standard density

T..... temperature

T_o.... reference temperature used in standard density

T_{MD}.. temperature of maximum density

x..... square root of concentration of all dissolved solids in Quesnel Lake

z..... depth

z'..... integration variable for depth used in quasi-density

z_r..... reference depth used in quasi-density and potential density

α..... coefficient of thermal expansion

β..... coefficient of haline contraction

γ..... temperature-dependent coefficient for compressibility

λ_i.... equivalent conductivity of ion i

λ_i^∞.... limiting equivalent conductivity of ion i

Λ..... equivalent conductivity of a salt

Ψ..... adiabatic lapse rate of density

ρ..... density

ρ_o .... mean density
ρ_{CM} .. density calculated with the equation of state developed by Chen and Millero (Chen and Millero, 1986)
ρ_{pot} ... potential density
ρ_{quasi} .. quasi-density
$\rho_{Quesnel}$ density calculated with the equation of state developed specifically for Quesnel Lake
σ ..... ρ-1000, [kg/m^3]
θ ..... potential temperature

List of Abbreviations

EOS_{CM} Equation Of State developed by Chen and Millero (Chen and Millero, 1986)
CTD .. Conductivity - Temperature - Depth probe
DDW . De-ionised Distilled Water
PESC . Pacific Environmental Sciences Centre
PVT .. Pressure Volume Temperature properties
EOS_{QL} Equation Of State developed specifically for Quesnel Lake

Acknowledgements

I would like to express my gratitude to the following people for their assistance in the completion of this thesis. I would like to thank Dr. Bernard Laval, my supervisor, who has been a great source of ideas and guidance through this process. I am very grateful to the researchers from the Institute of Ocean Sciences, Fisheries and Oceans Canada including Dr. Eddy Carmack, John Morrison and Dr. Svein Vagle who have helped me carry out my field work and develop some of the ideas presented here. Fellow students including Daniel Potts and Ryan North also helped with field work. Roger Pieters from the Department of Earth and Ocean Sciences, University of British Columbia spent much time discussing the finer points of this project with me. Thank you also to Dr. Svein Vagle of the Institute of Ocean Sciences, the Provincial Ministry of Water Land and Air Protection and Fisheries and Oceans Canada's Cultus Lake Laboratory for providing ship time. I was supported by Fisheries and Oceans Canada under the Science Subvention Research grant. Dr. Greg Lawrence from the Department of Civil Engineering, University of British Columbia also provided generous assistance in this project. I am also very thankful to Brock Wilson and Sabina and Douglas James, for their love through this process.

1 Introduction

Quesnel Lake is a part of the Fraser River system and is an important habitat for salmon. Historically, Quesnel Lake received up to one third of the entire Fraser River run of salmon as they spawn in the lake or pass through it on their way to their natal streams. This makes Quesnel Lake a gateway to the catchment which contributes the largest salmon population to the Fraser River watershed (Royal, 1966). After the rock slide at Hell's Gate in 1913, the salmon population in Quesnel Lake was reduced to the point where there were too few salmon to make observations (Thompson, 1945). In recent years, salmon escapement has returned to near record numbers increasing to 3.5 million in 2001 (Fisheries and Oceans Canada, 2001). Thus, a critical management issue concerns the lake's primary productivity, and the role lake mixing and convection plays in returning nutrients to the surface (euphotic) layer of the lake. The deep water of Quesnel Lake has oxygen levels near or at saturation suggesting that deep water is being ventilated by oxygenated surface water. Also, nutrients from bottom waters are, in some way, being recycled to the surface where these nutrients then support primary production. Therefore, a motivation for studying Quesnel Lake is to determine what mechanisms contribute to vertical mixing and deep water renewal and how these mechanisms affect the Quesnel Lake salmon resource.

Quesnel Lake, located on the western edge of the Cariboo mountains in British Columbia (BC), Canada, is a steep-sided fjord-type lake consisting of three long, narrow arms (Fig 1). With a maximum depth of 511 m, it is the deepest lake in BC and one of the deepest lakes in the world. It has a volume of approximately 41.5 km^3 and a surface area of 266.3 km^2. Quesnel Lake has three major in-flowing rivers, the Horsefly River, Mitchell River and Niagara Creek and one major outflow, the Quesnel River.

Conductivity - temperature - depth (CTD) profilers are routinely used for oceanographic and limnological research. These instruments measure the conductivity, temperature and pressure as they descend through the water column. In order to study

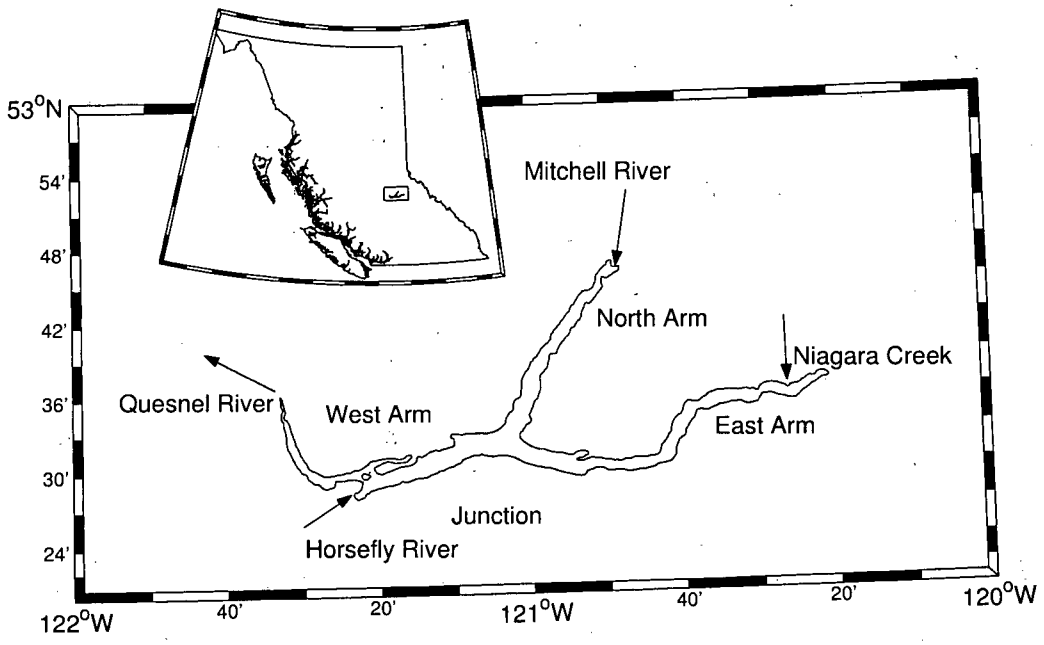

Figure 1: Map of Quesnel Lake. Data from Campbell (2001). Place names are used in text.

vertical mixing in Quesnel Lake, density profiles, calculated from in-situ CTD measurements, were used. To find density profiles from CTD data, a lake specific equation of state must be employed. The equation of state relates a fluid's density, ρ, to its temperature, T, salinity, S, and pressure, p:

$$\rho = \rho(T, S, p) \tag{1}$$

While T and p are both directly measured by a CTD, lake-specific relations are required to estimate salinity from in-situ measurements. Once a salinity relation has been established, a modified general equation of state (e.g. Chen and Millero, 1986) can be used to determine water column density. Regions of mixing can often be identified from density profiles by isolating sections where density inversions, and therefore instabilities, occur (Hohmann et al., 1997). Identifying where Quesnel Lake's

water columns become unstable is an integral part of understanding how this deep ($>$ 250m) lake mixes vertically.

This paper will describe the processes by which water samples were taken from Quesnel Lake and analysed in order to determine the lake-specific equation of state for Quesnel Lake, hereafter referred to as EOS_{QL}. Chapter 2 will outline work done by previous researchers on this topic. Chapter 3 will give detail about the field work that was carried out at Quesnel Lake along with the method by which the data was analysed. Chapter 4 will show the results of this analysis, namely the developed EOS_{QL}. Chapter 5 will investigate local stability using the EOS_{QL} and the Brünt-Väisäla Frequency in conjuction with CTD profiles and describe a proposed mechanism that is contributing to the deep water ventilation of Quesnel Lake.

2 Literature Review

This section presents a summary of other works that have addressed equations of state and local stability. In doing so, proceedures that are applied to Quesnel Lake water samples and CTD profiles are identified. Specifically, this section addresses other works related to equations of state (Section 2.1), the introduction of state variables (Section 2.2) and the specific issues related to each one, the developement of the relationships required to determine an equation of state (Section 2.3), and the strategies other researchers have used to investigate profile stability (Section 2.4).

2.1 Other Works related to Equations of State

In the ocean, the relative proportions of dissolved salts are nearly constant throughout the world (Lewis, 1980). Therefore, only one equation of state is required to characterise stability throughout the world's oceans. In contrast, the salinity in lakes may vary from lake to lake or even between different water masses within a lake (i.e., differences in salt content between the hypo-, meta- and epilimnion) (Wuest et al., 1996). Varying local geology and river inflow can contribute to differing ion ratios (Millero, 2000a; Gray et al., 1979) which can affect the relationship between measured salinity and calculated salinity. For this reason, there is no analogous universal equation of state for all lakes.

Compared to other deep lakes in the world, mixing processes in Quesnel Lake have received little scientific attention to date. With the similar motivation of understanding mixing processes, lake-specific salinity and density relationships have been developed by numerous researchers studying other deep lakes:

- Lake Baikal in Siberia (Hohmann et al., 1997), at 1632m, which is the deepest lake in the world and is located in the Baikal Rift Zone.
- Lake Malawi (Wuest et al., 1996), which is 700m deep and lies on the borders of Zambia, Tanzania Mozambique and Malawi, is also a rift lake and is the third

deepest lake in the world.

- Lake Issyk-kul (Vollmer et al., 2002b), which is 668m deep and is located in the Tien Shan mountains of Kyrgyzstan is the fifth deepest lake in the world.

- Crater Lake (McManus et al., 1992) in Oregon, which is 590m deep and is in the collapsed caldera of Mount Mazama. It has hydrothermal vents that introduce thermally and chemically enriched water. It is the deepest lake in the United States and the seventh deepest lake in the world.

- Island Copper Mine Pit (Fisher, 2002) on Vancouver Island, BC, Canada, which is 340m deep. It was initially filled with salt water but, due to the inflow of acid rock drainage and disassociation of ions from the pit walls, the water's chemical composition changed with time such that the practical salinity scale, developed for seawater, no longer applies. A time dependent salinity correction was developed to be used with the equation of state for seawater. Although the situation for this lake is fundamentally different from Quesnel Lake, Island Copper Mine Pit is mentioned here because similar principles were employed in developing its equation of state.

In these examples, the lake-specific equations are primarily determined from chemical analysis of water samples taken from the given lakes.

2.2 State Variables

As described by Eq. 1, the equation of state depends on three variables: T, S and p. This section will outline how density is affected by each, as well as describe some of the complications associated with them.

2.2.1 Temperature

Fig. 2 shows the dependence of density on temperature. Above 4°C, density generally increases with decreasing temperature. At zero salinity and at atmospheric pressure,

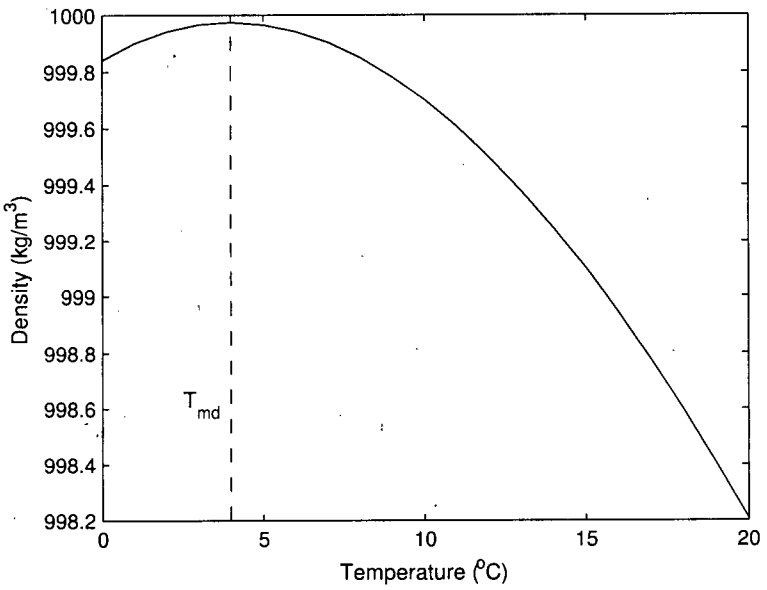

Figure 2: Dependence of density on temperature at atmospheric pressure and zero salinity. The vertical dashed line marks T_{MD}. This plot is based on the seawater equation of state given in Millero et al. (1980).

density reaches a maximum of 999.972 kg·m^{-3} at a temperature of 3.98°C. This is known as the temperature of maximum density, T_{MD}, and plays an important role in turnover in shallow (< 150 m) lakes. In shallow lakes, vertical mixing occurs when the stratification within the lake deteriorates due to temperature changes resulting from downward mixing of cooler surface water in spring and autumn. When the entire water column approaches 4°C, the stratification is reduced to the point of near uniform density. This loss of the water column stability results in seasonal turnover.

The temperature of maximum density, T_{MD}, has been a point of interest for other researchers in lake studies. In the early 1960s there was a short debate in Science between Eklund (1963, 1965) and Johnson (1964) relating to this subject. The focus was the Strom line (identified by Strom, 1945) which was incorrectly identified as T_{MD}. Eklund showed that T_{MD} is actually approximately 4^0C at the surface and has

a temperature gradient of -0.021^{o}C/bar (Eklund, 1963) whereas the Strom line is the temperature gradient at which a profile has maximum stability (Eklund, 1965). Another point of contention was whether or not temperature profiles could cross over the temperature of maximum density. Imboden and Wuest (1995) address this topic and show that profiles may pass over the temperature of maximum density if they have a positive slope when profile temperatures are greater than T_{MD} and a negative slope when profile temperature are equal or less than T_{MD}, as illustrated in Fig. 3.

Fig. 3 shows the change in T_{MD} with depth along with a theoretical winter temperature profile when reverse stratification occurs. Although the temperature profile crosses T_{MD}, it is stable. If, at any place in the profile, a water parcel was moved upwards, it would be heavier than the surrounding water (i.e. closer to T_{MD}) and would fall back to its original position. Conversely, if a water parcel was pushed downwards, it would be less dense as it would be further away from the T_{MD} line, and would return to its original position due to buoyancy forces. This is the condition for stability.

Other researchers have investigated the effects of T_{MD} on lake stability problems as it plays an integral role in several interesting mixing mechanisms. For example, T_{MD} plays a large role in the dynamics of thermobaric instabilities which have been studied by Sherstyankin and Kuimova (2002); Killworth et al. (1996) and Weiss et al. (1991). Thermobaric instabilities take place when wind or other external forcing pushes the cold water in the upper part of a reversely stratified water column down to where it is warmer than the local T_{MD}. If this occurs, the overlying water becomes denser than the underlying water, resulting in episodic, local mixing. See Weiss et al. (1991) for a detailed explanation. Cabelling, another phenomena that relies on the anomaly of T_{MD}, occurs when two water masses, one cooler than T_{MD} and one warmer, mix together to make heavier water with a temperature closer to T_{MD}. This heavier water then sinks and creates a plume of down-welling surface water called a thermal bar. Thermal bars occur when incoming river water or water near a lake's shore heats up while the bulk of the lake remains cold. A thermal bar can move across a lake

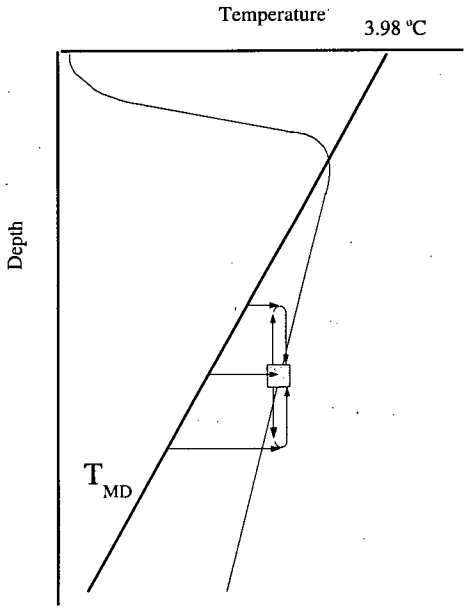

Figure 3: Illustration of a stable profile that crosses T_{MD}. Based on the seawater equation of state in Millero et al. (1980).

as the season changes. This phenomenon has been studied by researchers including Shimaraev et al. (1993), Carmack (1979b) and McDougall (1987).

T_{MD} effects do not cause complications in oceanic waters. Fig. 4, which shows how seawater T_{MD} (calculated using the equation of state for seawater extended to $T = -5.5°C$ for illustration purposes only) and seawater $T_{freezing}$ change with pressure. At the surface, the extrapolated T_{MD} is cooler than $T_{freezing}$. As pressure is increased, these values diverge. In waters with high ($> 24.7\ ^{o}/_{oo}$) salinity content (like in the bulk of the ocean) water will always freeze before it reaches its T_{MD}. For this reason, T_{MD} effects need not be considered. However, in fresh water like in Quesnel Lake, $T_{MD} > T_{freezing}$ making T_{MD} effects relevant.

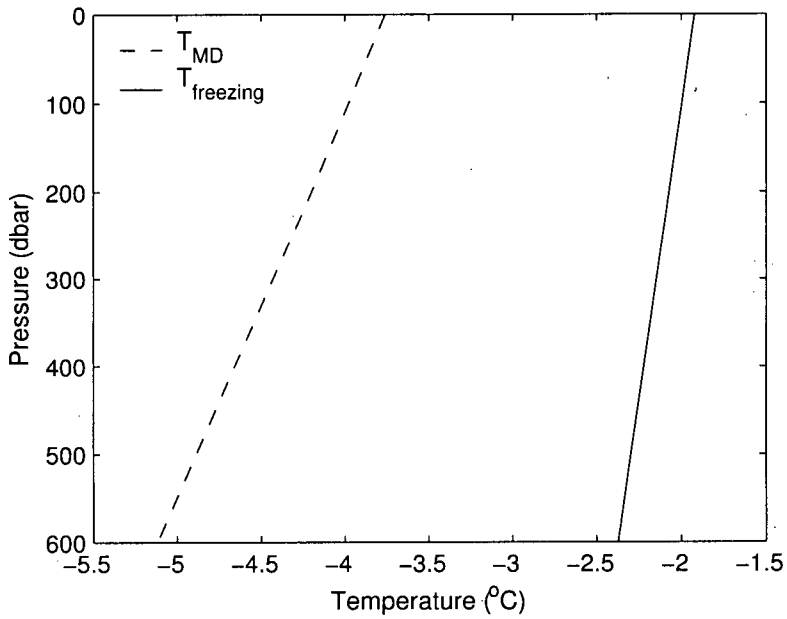

Figure 4: T_{MD} and $T_{freezing}$ for seawater at S=35 as a function of pressure.

2.2.2 Salinity

Often fresh water lakes are assumed to have zero salinity. Making this assumption can lead to errors when calculating the physical and chemical properties of lakes. This was first pointed out by Chen and Millero (1977a) in relation to mistakes made in estimating Lake Ontario properties under the assumption that the water had zero salinity. The average salinity in Lake Ontario is 0.209 $^{o}/_{oo}$ which, according to the equation of state developed by Chen and Millero (1976), is enough to depress T_{MD} by more than 0.04°C Chen and Millero (1977a).

Lake water salinity, the composition of dissolved solids, cannot be found by making one measurement alone. Only a fully detailed chemical analysis on a water sample can determine its salinity (Lewis, 1980). This process is too time consuming for routine use and consequently a simpler method must be developed in order to measure salinity throughout a water column. This is done by relating salinity to easily measured CTD

parameters.

For ocean water, CTD parameters are related to salinity using the practical salinity scale of 1978 (PSS78) (Dauphinee, 1980; Lewis, 1980; Hill et al., 1986). This relationship is based on extensive measurements conducted at five seperate laboratories (Dauphinee, 1980) and is the standard equation used to determine salinity in seawater. PSS78 determines a "practical salinity" based on measurements of the conductivity ratio, r, defined in Eq. 2 as the ratio of the conductivity of the sample to the conductivity of a standard potassium chloride solution (KCl) at S=35 and T=15 ^{o}C at atmospheric pressure (Lewis, 1980):

$$r = \frac{C(S,T,p)}{C(35,15,0)} \tag{2}$$

PSS78 assumes that all waters with the same conductivity ratio, r, have the same salinity. The original PSS78 equation is only valid for salinities in the range of 2 to 42. Hill et al. (1986) extended the validity of PSS78 to salinities between 0 and 2 by adding a correction term. However, this extended equation still only applies to waters with the same compositions as seawater.

Fig. 5 shows isopycnals of seawater with temperature and salinity changes to help illustrate density's dependence on salinity. At most temperatures the density of a lake's water is heavily dependent on the temperature of the water. However, in the temperature range near T_{MD}, $\frac{\partial \rho}{\partial T}$ approaches 0. In this range, changes in density are less sensitive to changes in temperature, and salinity effects may become important. The salt content of freshwater lakes must be considered when calculating density in deep lakes such as Quesnel Lake where much of the water has temperature near T_{MD} throughout the year (Fig. 6 a).

Millero (2000b) proposes that using the equation of state for seawater at low salinities for lake water with the same salinity is adequate. He argues that the changes in the properties of low salinity solutions are independent of the specific salt added because, when diluted, the ion-ion interactions of salts in solution are reduced. He compares relative density ($\rho_{in-situ} - \rho_{mean}$) calculated based on the composition of

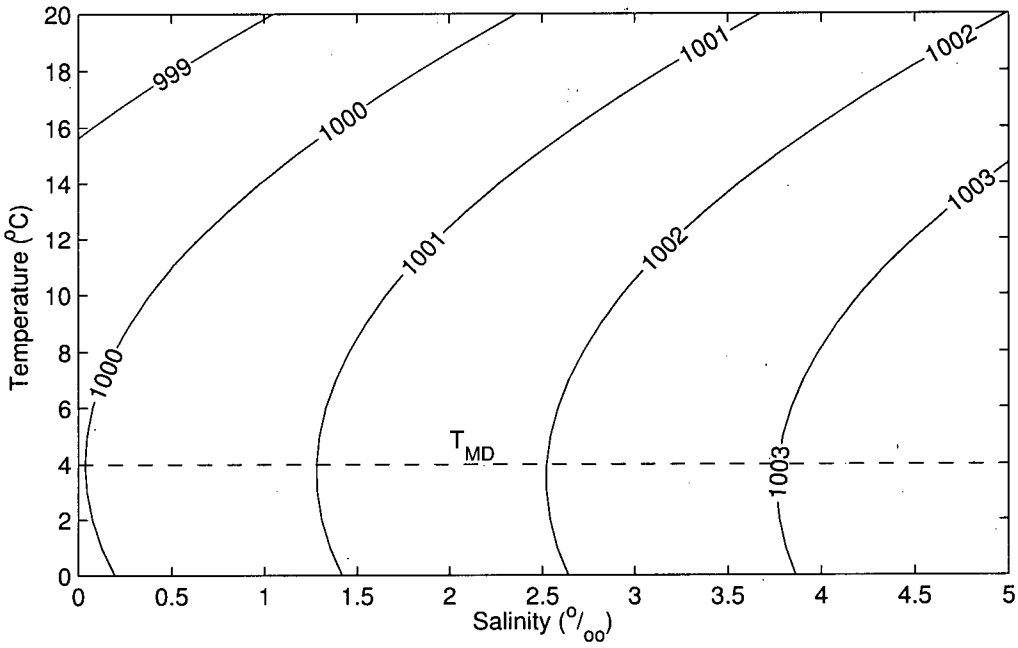

Figure 5: Plot showing the dependence of density on temperature and salinity using seawater at low salinities for illustration. The horizontal dashed line marks T_{MD}. Contour interval is $1kg/m^3$. This plot is based on the equation of state developed for the limnological range in Chen and Millero (1986) at atmospheric pressure.

Lakes Baikal (S=0.0963 $^o/_{oo}$), Malawi (S=0.205 $^o/_{oo}$), and Tanganyika (S=0.568 $^o/_{oo}$) with the relative density for seawater diluted to the same total salinity and finds that the values agree to within the error inherent in the seawater equations. He concludes that lake salinity can be taken to have the same composition as seawater diluted to the same concentration of total dissolved solids as the lake water being studied. This approach for brackish Lake Issyk-kul (S=6.06$^o/_{oo}$) was disputed by Vollmer (2002) who showed that, at this concentration, the proportion of the ions dissolved is important and so the composition of the lake must be considered.

In order to use any equation of state, a water body, ocean or lake, must have a composition with a constant proportion of concentrations. As the total concentration

of ions change, the individual ions dissolved in the water must change at the same rate in order to maintain constant proportionality of ions and apply an equation of state. Changes in conductivity must reflect changes in both ionic and non-ionic constituent concentrations. McManus et al. (1992) discuss the issue of constant relative composition in their study of Crater Lake. The concentration of silicic acid, a non-ionic constituent introduced to Crater Lake via submerged thermal vents, was compared to the concentration of a strong electrolyte (Na^+) meant to represent the lake's ionic salinity. McManus et al. (1992) showed that in Crater Lake silicic acid varies directly with ionic constituents and, therefore, variations in specific conductance will reflect the variations in overall concentration of dissolved solids. The proportional variation of ionic and non-ionic constituents is assumed in studies of other lakes (Vollmer et al., 2002b; Hohmann et al., 1997; Wuest et al., 1996). If this were not the case, the non-ionic contributors to salinity could not be parameterised in terms of easily measured quantities such as those measured by a CTD. The only alternative would be to measure non-ionic constituent concentrations directly.

2.2.3 Pressure

Pressure plays a role by mechanically increasing density due to compression. Because cold water is more compressible than warm water, T_{MD} decreases with increasing pressure. Fig. 6b shows the relationship between pressure and T_{MD}. In deep lakes, renewal processes may take longer than in shallow lakes because bottom water is constrained by the pressure dependence of T_{MD}. For example, as surface water cools below 4 ^{o}C, it will not mix downwards because it is less dense than water at T_{MD} below. Cool bottom water (i.e. $T < 4^o$C) will not mix upwards because it is closer to T_{MD} when under pressure. In this way, interaction between surface and bottom waters can be suppressed.

Small variations in the temperature profiles of Fig. 6b may or may not represent instabilities. The fluctuation in temperature may be compensated by a fluctuation in salinity resulting in a stable profile. Only with the use of an accurate equation of state

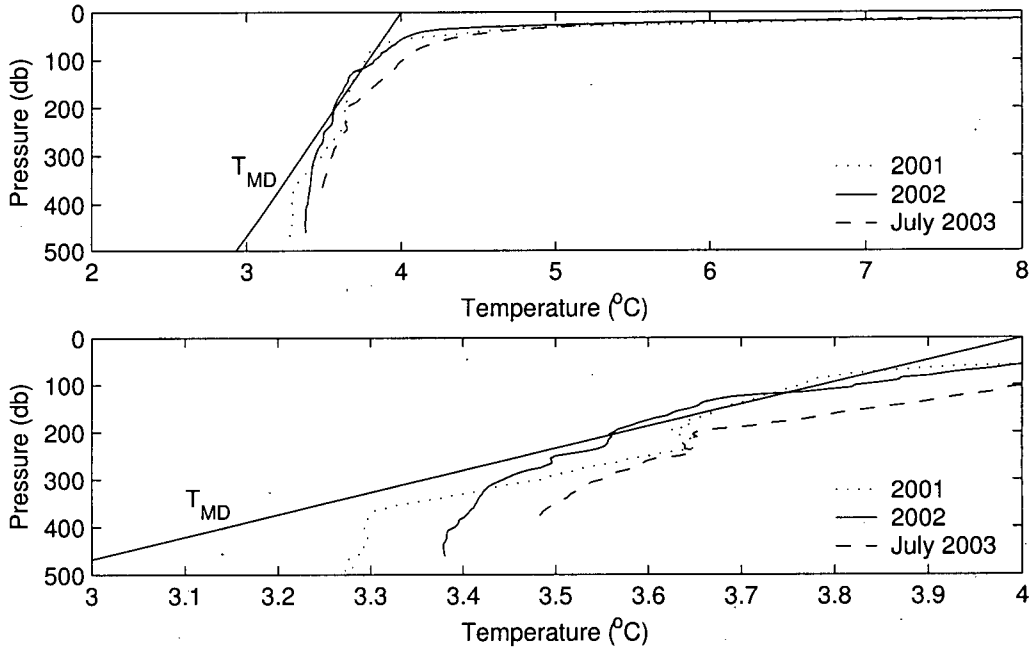

Figure 6: (a) Temperature profiles in East Arm of Quesnel Lake from 2001 to 2003. (b) Blow up of temperature profiles over temperature range of 3 to 4 °C.

can instabilities be identified. Once density profiles are established, quasi-density and the Brünt-Väisäla Frequency will be used to locate instabilities. In this way, mixing in Quesnel Lake can be analysed.

2.3 Relationships

2.3.1 Relating Conductivity to Specific Conductance

Conductivity, the ability of an aqueous solution to carry an electric charge, is dependent on the concentration of ions present, and on the temperature and pressure of the solution. Often, measured conductivity is converted to specific conductance at a reference temperature and pressure. Doing this removes the temperature and pressure signals and leaves only a conductivity signal that reflects the concentration

of ionic constituents. In North America, the reference temperature and pressure for specific conductance are $T = 25°C$ and $p = 0$ bar, respectively (Physical and Aggregate Properties, 2000). A conversion between the measured in-situ conductivity, C_T^P, to the specific conductivity, C_{25}^0, can be approximated by:

$$C_T^P = f_P \cdot f_T \cdot C_{25}^0 \tag{3}$$

where f_P is the temperature-dependent pressure correction, which accounts for the increase in conductivity due to compression of water, and f_T is the temperature correction, which accounts for the dependence of conductivity on temperature for a given composition (Wuest et al., 1996). This conversion is analogous to the conductivity ratio, r, used by oceanographers (Perkin and Lewis, 1980) (See Eq. 2).

Bradshaw and Schleicher (1965) experimentally determined an empirical relationship between pressure and the electrical conductance of seawater. Other researchers (e.g. Wuest et al., 1996; Hohmann et al., 1997) who have studied deep lakes have extended Bradshaw and Schleicher's formula to low salinities through linear extrapolation and applied it to their respective lake waters. In addition, Hohmann et al. (1997) experimentally verified the extrapolated values. The temperature and pressure sensors of a CTD were wrapped in plastic before it was lowered to keep the same water parcel throughout the depth of the profile. The change in electrical conductivity with pressure was measured directly. The experiment yielded pressure correction values that are remarkably close to the extrapolated values for the same parameter (Hohmann et al., 1997). In his study of Lake Issyk-Kul, Vollmer (2002) uses a pressure dependence that is developed specifically for this lake in order to eliminate small errors that are introduced by using equations developed for seawater. In the present study, for lack of a study that is more appropriate for describing pressure effects in lakes, the formula developed by Bradshaw and Schleicher (1965) extrapolated to low salinities was used to determine the pressure correction factor f_P, in the equation of state for Quesnel Lake.

The temperature correction depends on a lake's composition and so must be found

specifically for each lake. The temperature correction is determined by finding the ratio of conductivity at zero pressure, C_T^0, to C_{25}^0 over a range of temperatures, at a fixed pressure ($P = P_{atmospheric} = 0dbar$) and then fitting this data to a function. Researchers have found the temperature correction both experimentally and analytically. Gray et al. (1979) and Johnson (1989) did this experimentally by measuring the conductivity of a sample of lake water over a range of temperatures in a laboratory and then fitting the collected data to a function to find the form of f_T. Analytically, the temperature correction is determined by analysing a water sample for ionic composition, pH and alkalinity and using the collected data to calculate conductivity over a range of temperatures. This procedure was outlined in detail by Wuest et al. (1996) and used by Hohmann et al. (1997).

There are a variety of functions that can be used to fit the conductivity and temperature data. Standard methods suggest the following form for this relationship:

$$f_T = \frac{C_T^0}{C_{25}^0} = 1 + \alpha(T - 25) \tag{4}$$

where α is a temperature coefficient, calculated for individual water samples. Other forms that can be used are an exponential function (Gray, 1979) or, more commonly, a polynomial form (Wuest et al., 1996).

The analytical method will be applied to Quesnel Lake water samples over 0 to 25 °C, the natural temperature range found in Quesnel Lake and will be described in more detail in Section 3.

2.3.2 Relating Specific Conductance to Salinity

Rather than convert conductivity data to specific conductance, McManus et al. (1992) directly related salinity to temperature and in-situ conductivity using a least squares regression. A more common method is to relate salinity to specific conductance through one of two ways. For a dilute solution, a relationship between specific conductance and salinity is approximated to be linear (Sorensen and Glass, 1987) as was done for Arrow Lakes by Wuest (1999). Alternatively, if more precision is required,

a temperature dependent third order polynomial can be used as was done by Wuest et al. (1996) for Lake Malawi and Hohmann et al. (1997) for Lake Baikal. Quesnel Lake, which is ultra-oligotrophic, has ion concentrations that are low enough to make ion-ion interactions negligible and for this reason, salinity is assumed to be linearly related to conductivity.

2.3.3 Relating Salinity to Density

To calculate density in seawater, UNESCO (1981) recommends using the equation of state developed in 1980 (EOS80) for temperatures between -4 and 40 ^{o}C, pressures between 0 to 1000 bar and salinities between 0 to 40 $^{o}/_{oo}$. Developed separately, Chen and Millero (1977b) initially presented an equation of state suitable for limnological systems based on temperature and pressure effects of fresh water combined with seawater effects on salinity. This limnological equation of state assumes that a lake's salt composition is identical to that of seawater, but diluted to the same concentration (Chen and Millero, 1977b). This equation was modified to have a claimed accuracy better than 2 x 10^{-6}g$\cdot$ cm^{-3} and re-presented, along with relationships for other PVT properties such as thermal expansibility, isothermal compressibility and temperature of maximum density by Chen and Millero (1986). The equation of state presented by Chen and Millero (1986) specifically for the limnological range will hereafter be referred to as EOS$_{CM}$. EOS$_{CM}$, which was used by McManus et al. (1992) for Crater Lake, is valid for limnological ranges of temperatures between 0 and 30 ^{o}C, pressures between 0 and 1700 bars and salinities between 0 and 0.6 $^{o}/_{oo}$.

EOS$_{CM}$ does not consider the unique composition of lakes. Millero (2000a) later suggested that one possible way to deal with the differing composition of water is to use an existing equation of state for seawater composition with a correction in density for added solutes. Reseachers including Wuest et al. (1996) and Hohmann et al. (1997) have found corrections for their respective lakes by determining an adjusted coefficient of haline contraction and using it in EOS$_{CM}$. The coefficient of haline contraction,

β, defined by:

$$\beta = \frac{1}{\rho} \cdot (\frac{\partial \rho}{\partial S}) \tag{5}$$

describes the influence of salinity on density, i.e.:

$$\rho = \rho_o(1 + \beta \cdot S). \tag{6}$$

where ρ_o is the average density.

Wuest et al. (1996) found the coefficient of haline contraction for Lake Malawi at p=0 bar and T=25°C was 1.028 times greater than that found by EOS_{CM} due to the differing composition from dilute seawater. In calculations for density structure and stability, Wuest et al. (1996) use EOS_{CM} with $\beta^{Malawi} = 1.028 \cdot \beta^{Chen+Millero}$ in place of $\beta^{Chen+Millero}$. Hohmann et al. (1997) use the same method. The method outlined by Wuest et al. (1996) will also be applied to Quesnel Lake.

Density can also be measured directly. Fisher (2002) used density, measured with a densitometer, to back calculate the salinity of Island Copper Mine pit water samples. Grafe et al. (2002) showed that density can also be measured in-situ to an accuracy of *pm* 1 kg/m^3 with an ultrasonic pulse transmitted through a quartz glass cylinder and received by a piezo ceramic. Direct density measurements of Quesnel Lake water were done with a densitometer to verify the lake-specific relationships for salinity and density developed in this paper.

2.4 Profile Stability

Local vertical stability is described by Imboden and Wuest (1995) as a condition in which, if a water parcel is displaced isentropically by a small vertical distance, it returns to its original depth due to buoyancy forces. Because pressure plays a large role in determining in-situ density, profiles of density often increase monotonically simply because of the compressibility of water. In situ-density is not a good representation of stability because, if a water parcel experiences forcing (i.e. internal waves), it could be displaced vertically and its density would change due to pressure. This change in density in the displaced parcel could result in a non-monotonically increasing, or

unstable, density profile. In order to address water column stability, in-situ density is often converted into a quantity that allows for easy comparison of densities of water parcels experiencing different pressures. Three such quantities are described below.

2.4.1 Potential Density

Often, potential density, $\rho_{potential}$, the density a water parcel would have it if were moved isentropically from its original pressure to a reference pressure, is used to remove the compression effect on density and allow comparison of water parcels within a CTD profile (Stansfield et al., 2001; Wuest et al., 1996; McManus et al., 1996). For potential density, the integrated adiabatic lapse rate of the parcel between the original position and reference pressure is subtracted from the in-situ density.

$$\rho_{potential}(z, z_r) = \rho(z) - \int_z^{z_r} \Psi(z, z')dz' \tag{7}$$

where z is the depth (positive upwards), z_r is a reference depth, and Ψ is the adiabatic lapse rate for density of a water parcel undergoing isentropic transport, defined by:

$$\Psi(z_1, z_2) = -\{\frac{d\rho[\theta(z_1, z_2), S(z_1), p(z_2)]}{dz_2}\}_{isentropic.} \tag{8}$$

where θ is potential temperature, the temperature a water parcel would have it if were moved isentropically from its original pressure to a reference pressure. However, because potential density is a path-independent quantity, the second term reduces to two simple terms and the expression for $\rho_{potential}$ simplifies to:

$$\rho_{potential}(z, z_r) = \rho(z) + (\rho(S, \theta, 0) - \rho(z)) = \rho(S, \theta, 0) \tag{9}$$

2.4.2 Quasi-Density

Quasi-density, ρ_{quasi}, introduce by Peeters et al. (1996), also removes the compression effect on density. Peeters et al. (1996) define quasi-density as:

$$\rho_{quasi}(z, z_r) = \rho(z) - \int_z^{z_r} \Psi(z', z')dz' \tag{10}$$

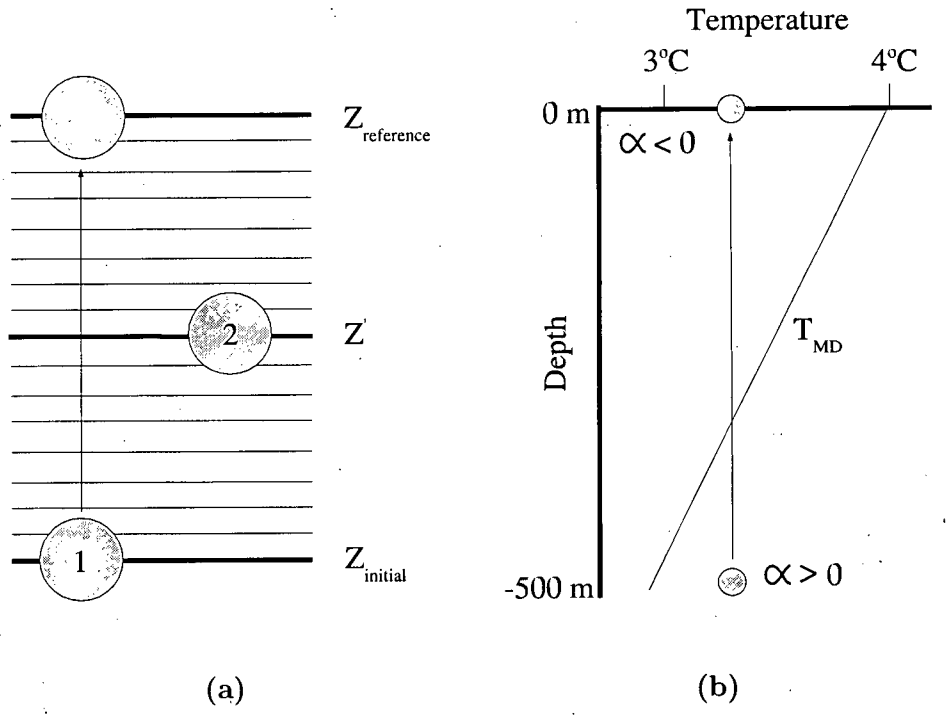

Figure 7: (a) Illustration of important variables for potential and quasi densities. (b) Illustration of water parcel being moved through T_{MD} when calculating potential density.

Quasi-density differs from potential density by comparing in-situ density with the integrated adiabatic lapse rate of the background water through which the parcel would pass if moved between the original pressure and a reference pressure. Fig. 7a illustrates the difference between potential density (i.e. if parcel 1 was moved to the surface without interacting with its environment) and quasi-density (i.e. if parcel 1 was moved to the surface while interacting with its environment such as parcel 2 at Z=Z'). Considering a parcel's interaction with its environment makes quasi-density path-dependent. A vertical path is assumed in its calculation. Quasi-density has no physical representation making it more difficult to conceptualise than potential density.

The reference depth often used in limnology and oceanography is the surface (i.e. $z_r = 0$). For potential density, a water parcel's density is determined at the surface which is equivalent to calculating the parcel's thermal expansion coefficient, $\alpha = \frac{1}{\rho} \cdot \frac{\partial \rho}{\partial T}$, at the surface:

$$\rho = \rho_o(1 + \beta S - \alpha T) \tag{11}$$

However, because α changes sign at T_{MD}, calculating a deep water parcel's α at the surface can cause sign errors to occur (Fig. 7b). Quasi-density takes into account the water surrounding the water parcel, and it's stability is determined locally so the sign errors, introduced in potential density, are avoided. Near T_{MD}, potential density is not adequate for determining stability (Ekman, 1934), whereas quasi-density gives accurate vertical structure in the water column (Peeters et al., 1996). Peeters et al. (1996) argues that quasi-density, is the quantity most appropriate for the comparison of density from various depths in deep lakes that reach temperatures near T_{MD}. Quasi-density was used by Hohmann et al. (1997) for Baikal and will be applied to Quesnel Lake CTD profiles in the present work.

2.4.3 Standard Density

Foster (1995) also introduced a quantity that removes the compressibility signal from in-situ density. Standard density, D, defined in Eq. 12, assumes that the measured water parcel's density's pressure dependence is linearly related to the pressure dependence of a reference water parcel. This is described by Foster's Eq. 1 replicated here:

$$D(S, T, P) = \rho(S, T, P) \cdot \frac{\rho(S_o, T_o, 0)}{\rho(S_o, T_o, P)} \tag{12}$$

where D is the depressurised standard density, S_o and T_o are the salinity and temperature of the reference water parcel respectively. Foster (1995) chose $S_o = 35$ and $T_o = 0°C$ which are close to the measured temperature and salinity of the water in his study. He also suggests that standard density should be used only for small ranges of temperature and uses standard density to investigate deep water formation in the Antarctic in the temperature range of -2 to +2 °C.

2.4.4 Brünt-Väisäla Frequency

The Brünt-Väisäla frequency, N, also known as the stability frequency, is the frequency at which a parcel will naturally oscillate if displaced from a position of neutral buoyancy. The stability, E, is proportional to N^2 and so is important in identifying where instabilities occur in the water column (Millard et al., 1990). N^2 is defined according to Eq. 13 (Imboden and Wuest, 1995).

$$N^2 = -\frac{g}{\rho} \cdot \frac{\partial \rho}{\partial z} \tag{13}$$

When $N^2 > 0$, the water column is stable, when $N^2 < 0$ the water column is unstable (Gill, 1982). Millard et al. (1990) describes various common ways of calculating N^2 from CTD measurements and compares the results. Peeters et al. (1996) calculated the Brünt-Väisäla frequency according to its definition (Imboden and Wuest, 1995) using quasi-density in the place of potential density (Eq. 14).

$$N^2 = -\frac{g}{\rho_{quasi}} \cdot \frac{\partial \rho_{quasi}}{\partial z} \tag{14}$$

Because quasi-density provides only local stability information, the Brünt Väisäla frequency calculated with quasi-density also only provides information on local stability. By taking the derivative of ρ_{quasi} with z, the following expression is found (Eq. 24 from Peeters et al. (1996)):

$$-\frac{d\rho_{quasi}}{dz} = (\frac{d\rho}{dz})_{isen} - \frac{d\rho}{dz} \tag{15}$$

Term 1 on the right hand side is the change in density with depth, or adiabatic lapse rate of density, of a parcel of water moved a finite distance isentropically through the water column. It is compared with term 2 on the right hand side which is the adiabatic lapse rate of density of the surrounding water moved the same distance. Fig. 8 helps to illustrate the stability criteria. If the change in density of the water parcel (term 1 in Eq. 15) over the distance Δz due to a change in pressure is smaller than the change in density of the surrounding water (term 2 in Eq. 15), the parcel

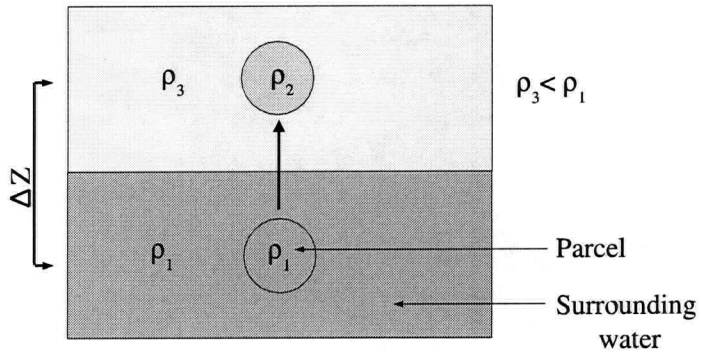

Figure 8: Schematic of Brünt Väisäla frequency, N^2. If a water parcel is moved, its change in density due to a change in pressure must be smaller than the change in density of the surrounding water for the parcel to be stable and have a positive N^2 value.

will be forced back to its original position due to buoyancy forces. This situation is considered stable and leads to a positive value for N^2. Note, $\frac{\Delta\rho}{\Delta z}$ is a negative quantity since density increases as depth decreases.

Peeters et al. (1996) calculated the Brünt Väisäla frequency from quasi-density values which had been averaged into 10 dbar bins. They discuss the merits of choosing a moderately sized bin; a bin size that balances resolving small instabilities, with having a noisy signal for N^2 with large errors.

3 Methods

3.1 Water Samples

Between July 23rd and 25th 2003, water samples were collected at locations around Quesnel Lake in order to determine the quantities necessary to estimate the lake's equation of state. Stations were selected with an attempt to sample every limnion. Water composition throughout the lake was sampled in order to test if the proportions of salts is constant as required by the theory presented in Section 2.2.2.

Samples were taken at each of the incoming rivers, Mitchell River, Horsefly River and Niagara Creek, as well as at stations in each arm that would be representative of that arm (Fig. 9). At each of these lake stations, samples were taken at the surface, at depth (near the bottom at that station) and at one or two depths in between. This was done to acquire samples representative of each strata at each station. In the East Arm, the deepest station, additional water samples (a total of 4) were taken in order to gain increased vertical resolution. Table 1 summarises the water samples taken in July, 2003.

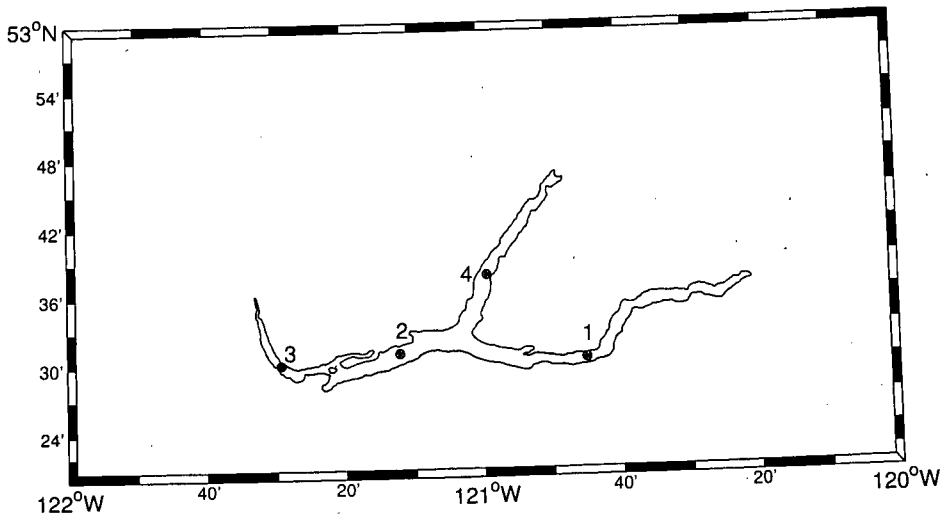

Figure 9: Map of water sample stations, Jule 2003.

Table 1: Depth (m) of Quesnel Lake water samples taken in July 2003. See Fig 9 for station locations.

Station 1	Station 2	Station 3	Station 4	Rivers
10	10	10	50	surface
125	110	85	100	samples
350	160		125	only
485				

Water samples were collected at 3 depths concurrently using cascading 1.71 L Niskin bottles. From each Niskin a 250mL acid washed polyethelene bottle was filled and the sample was acidified to a pH of less than 1.5 with Nitric acid in order to prevent metals from precipitating or absorbing into the container. Also, a 1L polyethelyne bottle was filled as full as possible with remaining water. The 1L bottles were on average 2/3 full.

After being collected, water samples were sent to the Pacific Environmental Sciences Centre (PESC), an analytical chemistry lab in North Vancouver, British Columbia. PESC was requested to perform a variety of tests on the collected water samples. These test fall into two categories: physical properties and concentration of constituents, summarized in Table 2.

In the development of a specific conductance relationship for in-situ CTD measurements, the conductivity of Quesnel Lake water over a range of temperatures is required. The 10 ions present in Quesnel Lake water in greatest concentration are used in this analysis. The contribution to conductivity of ions present in very small amounts ($< 5\%$ of total concentration of ionic constituents) is negligible compared to the contribution of the major ions. The results obtained from PESC are summarized in Fig. 10 which displays the distribution of concentration of the 10 dissolved ions with greatest concentration in Quesnel Lake based on the 15 water samples collected in July 2003.

In July 2003, surface water samples were also collected in 4L polyethelyne bottles

Table 2: Summary of analytical chemistry test performed on Quesnel Lake water samples collected in July 2003.

Quantity	Method	Samples
pH	Liquid Junction Potential	all samples
Alkalinity	electrometric titration	
specific conductance	conductivity meter	
Anions	Ion Chromatography (ICA)	all samples
Cations	Inductively Coupled Plasma Spectrometry (ICP)	
Nitrate/Nitrite	Colorimetry	all samples
Ammonium	Colorimetry	
Orthophosphate	Colorimetry	
Total dissolved phosphate	Colorimetry	surface and deep samples in East Arm
Total phosphate	Ascorbic Acid Reduction and Colorimetry	

at each of the stations in Quesnel Lake. Additional water samples were collected on June 22nd and 23rd, 2004 for the purpose of verifying the density estimates of EOS_{QL}. These water samples were taken in the East and North Arms (Fig. 11) with a 1.71L Niskin bottle primarily at a depth of 30m although some adjustments were made due to the shallower bottom depth at some stations. Table 3 summarises the water samples taken in June, 2004.

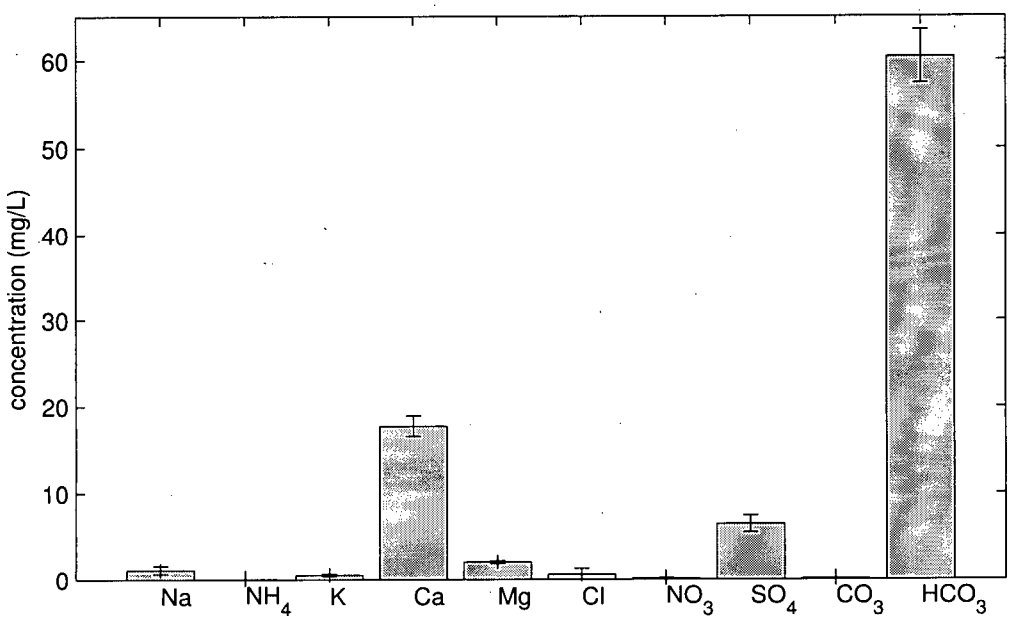

Figure 10: Average concentrations and standard deviations of the 10 ions with greatest concentration in Quesnel Lake in July 2003.

3.2 Calculating Conductivity

By summing the conductivities of individual ions, the conductivity for a water sample can be calculated. For ionic constituents, the sample conductivity is given by:

$$C_T^0 = \sum_{i=0}^{N} C_i \tag{16}$$

where C_i is the conductivity of ion, i.

Equivalent conductivity, λ_i, is the conductivity per ion equivalent at finite dilution and must be multiplied by the ion's concentration to determine the conductivity contributed by that ion. The relationship between an ion's conductivity, C_i, the ion's equivalent conductivity (at finite dilution), λ_i, and the ion's concentration, c_i, is given by:

$$C_i = \lambda_i \cdot c_i \tag{17}$$

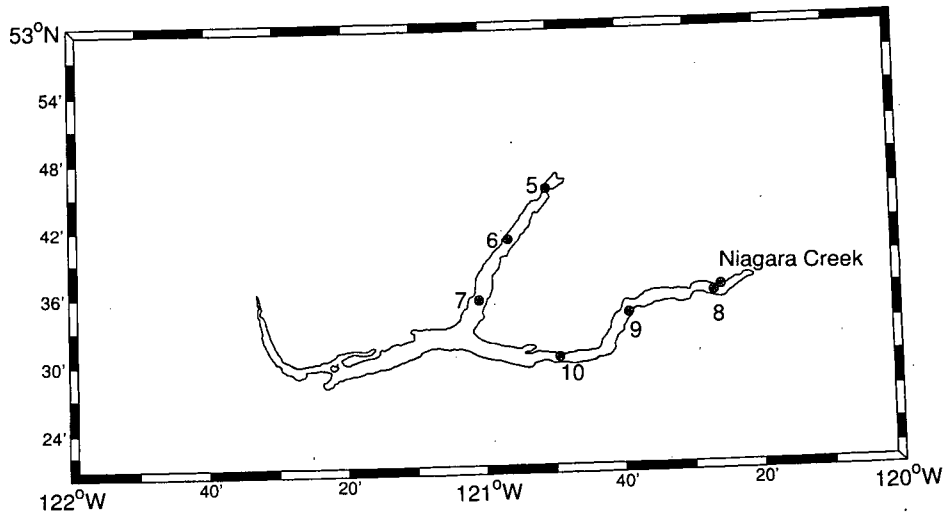

Figure 11: Map of water sample stations, June 2004.

Table 3: Depths of Quesnel Lake water samples taken in June, 2004

Station 5	Station 6	Station 7	Station 8	Station 9	Station 10	Niagara Creek
20	30	30	30	30	30	surface
20	30	30	30	30	30	surface

where conductivity is in units of $\mu S \cdot cm^{-1}$.

Onsager's equation describes the concentration dependence of λ_i in terms of the limiting equivalent conductivity (an ion's equivalent conductivity at infinite dilution), λ_i^{∞}, and sample concentration (Noggle, 1989).

$$\lambda_i = \lambda_i^{\infty} + k \cdot \sqrt{c} \tag{18}$$

At infinite dilution, the distance between nearest neighbouring ions is large, and the effect of the electric field due to surrounding ions is not felt. The limiting equivalent conductivity is a temperature and ion dependent quantity. Its dependence has been determined for ions that contribute significantly to Quesnel Lake's conductivity by

fitting empirical data (e.g. Robinson, 1959) to a third order polynomial. Fig. 12 (a) shows the fit of limiting equivalent conductivity for calcium as an example. Appendix A.2 shows the coefficients for the polynomial fit of the limiting equivalent conductivity for the top 10 ions dissolved in Quesnel Lake.

Introducing a new variable f_i — a reduction coefficient that takes into account the finite concentration of dissolved solids - Onsager's equation can be rewritten as follows:

$$\lambda_i = \lambda_i^{\infty} \cdot f_i \tag{19}$$

where the λ_i has units of $\mu S \cdot cm^{-1} \cdot eq^{-1}$ and

$$f_i = 1 + \frac{k \cdot \sqrt{c}}{\lambda_i^{\infty}} \tag{20}$$

As the distance between neighbouring ions decreases, the electric field applied on an ion due to its proximity to other charges retards the ion's motion. The reduction coefficient is a factor that quantifies the proportion by which the conducting capacity of an individual ion is reduced at finite dilution. Although the functional form of f_i is unique for each ion, it depends on the equivalent concentration of the entire solution. This assumes the conducting capacity of a given ion is influenced by the presence of all other charges in the solution irrespective of its origin. It is assumed that the proportion of ion concentrations in a lake's water is constant within that lake in both time and space. Therefore, the concentration dependence needs only to be found once and incorporated into the temperature correction which will be used in developing the equation of state that describes density throughout Quesnel Lake.

Kolhrausch's Law of independent migration of ions says that, at low concentrations, the equivalent conductivity of a solution, Λ, is given by the sum of the equivalent conductivities of its cationic and anionic contributors:

$$\Lambda = \lambda_+ + \lambda_- \tag{21}$$

The equivalent conductivity contributed by each ion in a salt is proportional to the ion's molecular mass. One can find the equivalent conductivity of an ion over a range

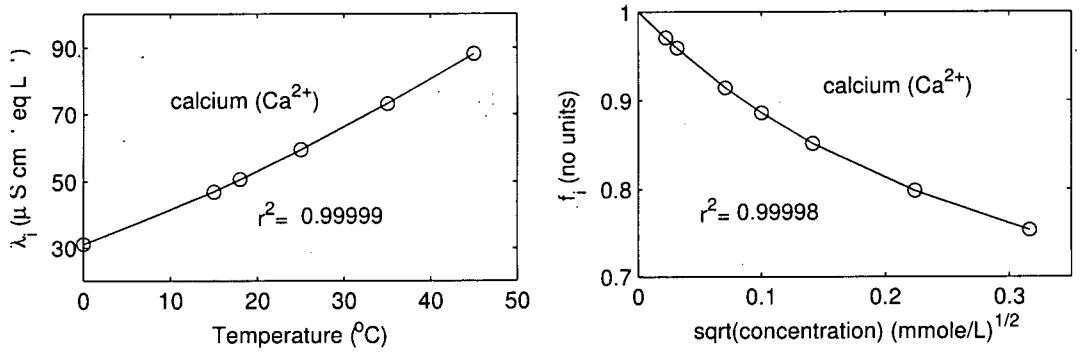

(a) (b)

Figure 12: Polynomial fits for calcium of (a) limiting equivalent conductivity over a range of temperatures, (b) the reduction coefficient over a range of concentrations.

of concentrations using published data for salts (Robinson, 1959; or Dean, 1979) at a reference temperature. Then, by dividing each ion's equivalent conductivities with its limiting equivalent conductivity at that temperature, one can develop a data set over which to fit a function in terms of the square root of concentration to obtain a concentration dependent form of f_i. This method has been implemented using a third order polynomial for all the ions of interest in Quesnel Lake. Fig. 12 (b) shows the fit for calcium as an example. Appendix A.2 shows the coefficients for the polynomial fit of the reduction coefficient for the top 10 ions dissolved in Quesnel Lake.

By substituting Eq. 19 into Eq. 17, one arrives at:

$$C_i = c_i \cdot \lambda_i^\infty \cdot f_i \tag{22}$$

Eq. 22 shows that the conductivity contributed by each ion is the product of the ion's equivalent concentration, its limiting equivalent conductivity and the reduction coefficient. The ion's concentration is measured directly by PESC, and the tempertaure dependence of the limiting equivalent conductivity and concentration dependence of the reduction coefficient are determined based on published data allowing conductivity to be calculated for Quesnel Lake water over a range of temperatures. These

conductivities are used to find a relationship for f_T which is described in Section 2.3.1 and used in Eq. 3 to find a lake-specific function for in-situ C^0_{25} in terms of CTD parameters.

3.3 Finding Salinity

By assuming that the ratio of specific conductance, C^0_{25}, to S is constant for a given lake (Section 2.3.2), the ratio of C^0_{25} to S found from Quesnel Lake samples can be related to the ratio of C^0_{25} to S measured in-situ with a CTD at Quesnel Lake in the future. This is illustrated with the following equation:

$$\frac{S_{sample}}{C^0_{25_{sample}}} = \frac{S_{CTD}}{C^0_{25_{CTD}}} = A \tag{23}$$

where

S_{sample} = total dissolved solids in the Quesnel Lake samples, [mg $\cdot$ L^{-1}],

$C^0_{25_{sample}}$ = sample's measured specific conductance, [μS $\cdot$ cm^{-1}],

$C^0_{25_{CTD}}$ = in-situ specific conductance calculated from CTD output, [μS $\cdot$ cm^{-1}],

S_{CTD} = in-situ salinity - the quantity for which an expression will be derived, [mg $\cdot$ L^{-1}]

A = lake-specific constant of proportionality found empirically from sample data.

To use Eq. 23 to find salinity in terms of CTD measurements, the empirical constant, A, is required for use with the lake-specific function for in-situ specific conductance described in Section 3.2.

The value of the empirical constant for Quesnel Lake was determined from the samples collected over the summer of 2003. The salinity is calculated by summing the mass contributed by each dissolved solid in a sample. This includes acids such as carbonic acid and its equilibrium components, bicarbonate and carbonate, which

were not measured directly but can be calculated indirectly from measurements of pH and alkalinity (See Appendix B). Also, non-ionic constituents must be included in the calculation of salinity since, although they do not contribute to conductivity, they do contribute to density. In order to include non-ionic constituents, one must assume that the ionic and non-ionic components vary proportionately. This assumption will be further discussed in Section 4.

The salinity is the sum of the mass of each dissolved constituent (including both ionic and non-ionic), and is given by:

$$S = \sum_i m_i \tag{24}$$

where m_i is the concentration of the dissolved constituent i and the units for salinity are mg $\cdot$ L^{-1}.

The constant A is determined by finding the ratio of salinity to specific conductance. The value of A is the slope of the best fit line that passes through the origin found using a least squares fit.

3.4 Determining the Coefficient of Haline Contraction

The coefficient of haline contraction, β, which describes how density changes with salinity was found using the procedure described by Wuest et al. (1996). Wuest's Eq. 12(b) for β, derived from the definitions of density and the haline contraction coefficient, is replicated here:

$$\beta = 1 - \frac{\rho \sum_i v_i c_i}{\sum_i M_i c_i} \tag{25}$$

where c_i is the ion's concentration, M_i is the ion's molar mass, and v_i is the ion's specific volume, the change in volume due to an addition of a salt. Specific volume describes the expansion and contraction of water due to dissolved salts. Although specific volume is a property of individual ions, specific volume data is only available for concentrations of salts (i.e. paired ions) (Millero et al., 1977). Therefore, ions dissolved in Quesnel Lake must be combined into salts stoichiometrically to use the

available data. Since specific volume is a property of the ion, it makes no difference which salts are made as long as all ions present in the sample are accounted for through this process.

The coefficient of haline contraction for Quesnel Lake was calculated based on the average composition of the 15 samples collected in July 2003. Table 4 shows how ions were combined stoichiometrically. The sum of charges, shown in Table 4, is used as a check to make sure anion and cation concentrations balance. Here, the balance is less than 3% of the total concentration of anions indicating that nearly all ions are accounted for in this method. Wuest et al. (1996) Eq. 12(b) is applied on the concentration of the assembled salts present in Quesnel Lake water to determine $\beta_{Quesnel}$.

Table 4: Stoichiometric combination of ions needed for determining the coefficient of haline contraction.

Ion	HCO_3	CO_3	SO_4	Cl	Ca	Mg	Na	K
Conc. [meq/L]	0.990	0.002	0.133	0.015	0.884	0.165	0.048	0.013
Salts								
Na_2SO_4			0.045				0.045	
NaCl				0.003			0.003	
KCl				0.013				0.013
$MgCO_3$		0.002				0.002		
$Mg(HCO_3)_2$	0.106					0.106		
$Ca(HCO_3)_2$	0.884				0.884			
$MgSO_4$			0.057			0.057		
Balance	0	0	0.032	0	0	0	0	0
Cations = 1.141 meq/L Anions = 1.109 meq/L Balance = 0.032 meq/L								

The coefficient of haline contraction effect on density can be expressed according to Eq. 26.

$$\rho = \rho_o \cdot (1 + \beta S - \alpha T)\rho = \rho(T) \cdot (1 + \beta \cdot S) \tag{26}$$

The second term in Eq. 26 adds a salinity correction to the original density. EOS_{CM} was used as a starting point for Quesnel Lake's equation of state. EOS_{CM} has the same structure as Eq. 26:

$$\rho_{CM} = \rho(T) \cdot (1 + \beta_{Chen+Millero} \cdot S) \tag{27}$$

where ρ_o and $\beta_{Chen+Millero}$ are functions of temperature and pressure and S is a function of temperature, pressure, and conductivity. It is assumed that $\beta_{Quesnel}$ varies proportionally to $\beta_{Chen+Millero}$ (Eq. 28).

$$\beta_{Quesnel} = B \cdot \beta_{Chen+Millero} \tag{28}$$

Once related to $\beta_{Chen+Millero}$, $\beta_{Quensel}$ can be used in substituted into EOS_{CM} (illustrated in Eq. 29) to get EOS_{QL}.

$$\rho_{Quesnel} = \rho_o(1 + B \cdot \beta_{Chen+Millero} \cdot S) \tag{29}$$

3.5 Measuring Density

Density of water samples taken in 2003 and 2004 were measured directly using an Anton Paar DMA 5000 densitometer. The densitometer readings were used to quantify the error present in the EOS_{QL}. The Anton Paar densitometer determines the resonant frequency of the water by oscillating the sample. The resonant frequency is inversely proportional to the root of water's mass. From the mass and the known volume (1.5mL) into which the sample is injected, the densitometer calculates the sample's density.

Water samples were injected into the densitometer by syringe. Before using the syringe, the syringe's tip was rinsed with the sample water to be measured and dried. Then, the syringe body was rinsed with the sample water 4 times. The densitometer cell was also rinsed with 5.5mL of the sample. As the sample was being injected into the densitometer, the cell was watched in order to assure no air bubbles were pushed into the cell. The densitometer then automatically warmed or cooled the sample to

20.000±0.001°C. Densities for Quesnel Lake water samples were found at atmospheric pressure.

Deionized, distilled water (DDW) was run through the machine at the beginning and end of each day as well as periodically throughout the time the measurements were being made in order to assure the offset of measured values was low and that drift in values was maintained at a minimum. When drift in baseline measurements exceeded 5 ppm, the Anton Paar densitometer was cleaned using its automated cleaning process and DDW was again measured to assure baseline values within 5ppm were attained.

3.6 CTD Profiles

Conductivity, temperature and depth (CTD) profiles presented here were taken during the summers of 2001 to 2003. Each summer, a different profiler was used. Data from 2001 and 2002 was collected by a team from the Institute of Ocean Sciences made up of Dr. Fiona McLaughlin, Dr. Mike Foreman, and John Morrison. In July 2003, CTD profiles were taken at each of the stations where water samples were collected (Fig. 9), as well as one in the junction (Fig. 1) using a Sea-Bird Electronics Inc. SBE 19 CTD profiler.

The SBE 19 used in 2003, had a sample period of 0.5s, and a resolution of ±0.0008°C in temperature, ±0.175 μS/cm in conductivity and ±0.09 dbar in pressure. The CTD was used in narrow conductivity mode to work in low salinity water. Only the CTD down-casts were used in quasi-density and N^2 calculations.

3.7 Applying Quesnel Lake's Equation of State

3.7.1 Quasi-Density

Analysis of vertical mixing requires that in-situ density profiles, which are dominated by hydrostatic pressure, be converted into a quantity that allows water parcels to be compared within a profile. Quasi-density profiles were found from CTD profiles, based on EOS_{QL}, using the procedure described by Peeters et al. (1996).

CTD data were sorted so that only the downcast was used and pressure was always increasing. Data collected in error was removed from the data set. Where two or more measurements were taken at the same depth, data was averaged so that each pressure had a unique set of C and T measurements.

Quasi-density was then calculated from the following algorithm which was executed for each measurement (i) in the CTD cast. Each calculation of quasi-density requires 3 data points ($i-1$,i,$i+1$).

Line 1: $\theta_1 = \theta(S_{i-1}, T_{i-1}, P_{i-1}, P_i)$

Potential temperature was determined over the whole water column using data point, $i-1$, the initial pressure and the measurement directly above it, i, as the reference pressure.

Line 2: $\sigma_{11} = EOS_{QL}(S_{i-1}, T_{i-1}, P_{i-1})$

In-situ density was determined using EOS_{QL} for each measurement, $i-1$, in the CTD cast.

Line 3: $\sigma_{12} = EOS_{QL}(S_{i-1}, \theta_1, P_i)$

Density was also determined using EOS_{QL} for the measurement directly above $i-1$, at i, as though the parcel at $i-1$ had been lifted isentropically (without change in heat or salt) to the pressure at i. For this reason, the density is found using the salinity at $i-1$, and the potential temperature, θ, as if the parcel was lifted to P_i with no heat loss.

Line 4: $(\frac{\partial \rho}{\partial z})_{i-1} = \frac{\sigma_{12}-\sigma_{11}}{z_i - z_{i-1}}$

In order to find the local adiabatic lapse rate for density (defined in Eq. 8), the change in density with depth was found for two adjacent depth intervals and averaged together to find the adiabatic lapse rate at i.

Line 5: $\theta_2 = \theta(S_i, T_i, P_i, P_{i+1})$

Line 6: $\sigma_{21} = EOS_{QL}(S_i, T_i, P_i)$

Line 7: $\sigma_{22} = EOS_{QL}(S_i, \theta_2, P_{i+1})$

Line 8: $(\frac{\partial \rho}{\partial z})_i = \frac{\sigma_{22} - \sigma_{21}}{z_{i+1} - z_i}$

Lines 6 through 9 are a repetition of line 2 through 5 with measurements at i and $i+1$ to find the adiabatic lapse rate for density at the second depth.

Line 9: $integrand(i) = \frac{(\frac{\partial \rho}{\partial z})_{i-1} + (\frac{\partial \rho}{\partial z})_i}{2} \cdot \frac{z_{i+1} - z_{i-1}}{2}$

In each iteration, one value for $\frac{\partial \rho}{\partial z} dz(i)$ is determined and added onto the end of the $\frac{\partial \rho}{\partial z} dz$ vector. In this way, computation time is saved because $\frac{\partial \rho}{\partial z}$ throughout the whole water column is not calculated in each iteration.

Line 10: $X = \sum(integrand)$

All entries in the integrand vector were summed to integrate the adiabatic lapse rate of density using the trapezoidal rule for integration (See Press et al., 1987).

Line 11: $\rho_{quasi_i} = EOS_{QL}(S_i, T_i, P_i) - X$

Finally, ρ_{quasi} was calculated by subtracting the integrated adiabatic lapse rate from the in-situ density. This was repeated until ρ_{quasi} was calculated for each point throughout the profile.

3.7.2 Standard Density

Throughout this paper, standard density is calculated according to the definition presented in the paper written by Foster (1995) and replicated here in Eq. 12.

3.7.3 Brünt Väisäla Frequency

The Brünt-Väisäla frequency is used to investigate water column stability from CTD profiles. It is calculated according to its definition (Imboden and Wuest, 1995) using quasi-density in place of potential density (Eq. 14) as recommended by Peeters et al.

(1996). Quasi-density was calculated using EOS_{QL} and the algorith presented in Section 3.7.1.

Without bin averaging CTD data, the N^2 profile contains a lot of information and is very noisy. In order to remove the noise, quasi-density data was smoothed through bin averaging. Bin averaging was performed before N^2 was calculated because, otherwise, the quasi-density gradient found from data points taken closer together (ie with minimal spacial resolution) are disproportionately large. The size of bin chosen for averaging is important. When averaging is done, information about N^2 is lost, and, simultaneously, the error in N^2 is reduced. The bin size must be chosen in a way that balances resolving structure of interest in the profile and maintaining a small enough error so that the signal that is resolved is meaningful. This compromise is also discussed by Peeters et al. (1996).

The error introduced through bin averaged ρ_{quasi} is estimated by finding the sum of the squares of the error in each bin as follows;

$$\delta\rho_{quasi} = \frac{1}{N-1}\sum_{i}^{N}(\rho_{quasi_i} - \overline{\rho_{quasi}})^2 \tag{30}$$

where N is the number of values of ρ_{quasi} in the bin, ρ_{quasi_i} is each value of ρ_{quasi} in the bin, and $\overline{\rho_{quasi}}$ is the mean value of ρ_{quasi} in the bin. This approach assumes that all values of ρ_{quasi} are without error and the error introduced is done so because the information contained in the bin averaged data is lost.

After N^2 is calculated, its error, δN^2, is estimated according to

$$\delta N^2 = \frac{g}{\rho_{quasi}\cdot\Delta z}\cdot\sqrt{2}\cdot\delta\rho_{quasi} \tag{31}$$

This approach assumes that the error contributed to δN^2 from Δz is negligible compared to the error contributed by $\Delta\rho_{quasi}$.

4 Quesnel Lake's Equation of State

4.1 Equation for f_T

In order to have an equation that describes the whole lake, one must assume that the conductivity reflects the total concentration of dissolved solids. Non-ionic constituents, such as silicic acid, must be factored into this equation. This is done by assuming concentrations of non-ionic constituents is proportional to concentrations of ionic-constituents. To test this assumption for Quesnel Lake, the concentration of silicon (Si) and a strong electrolyte present in Quesnel Lake, calcium (Ca) are compared (Fig. 13).

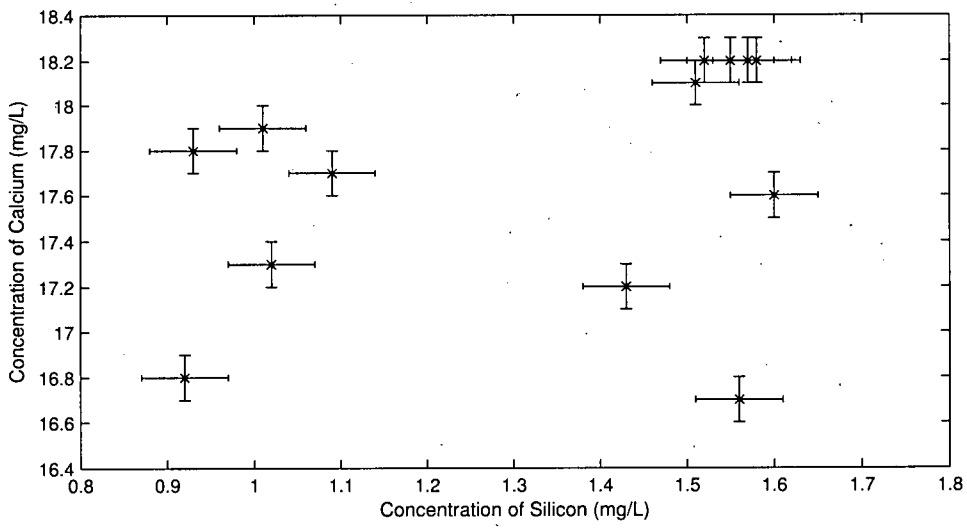

Figure 13: Concentration of silicon (Si) versus calcium (Ca) for 15 samples taken from Quesnel Lake July, 2003.

If Si and Ca varied proportionately, the data would fall on a line that passed through the origin. However, some variability is present in this data. The alternative to making this assumption would be to make direct measurements of non-ionic constituents with each CTD cast. This is prohibitively expensive and time consuming.

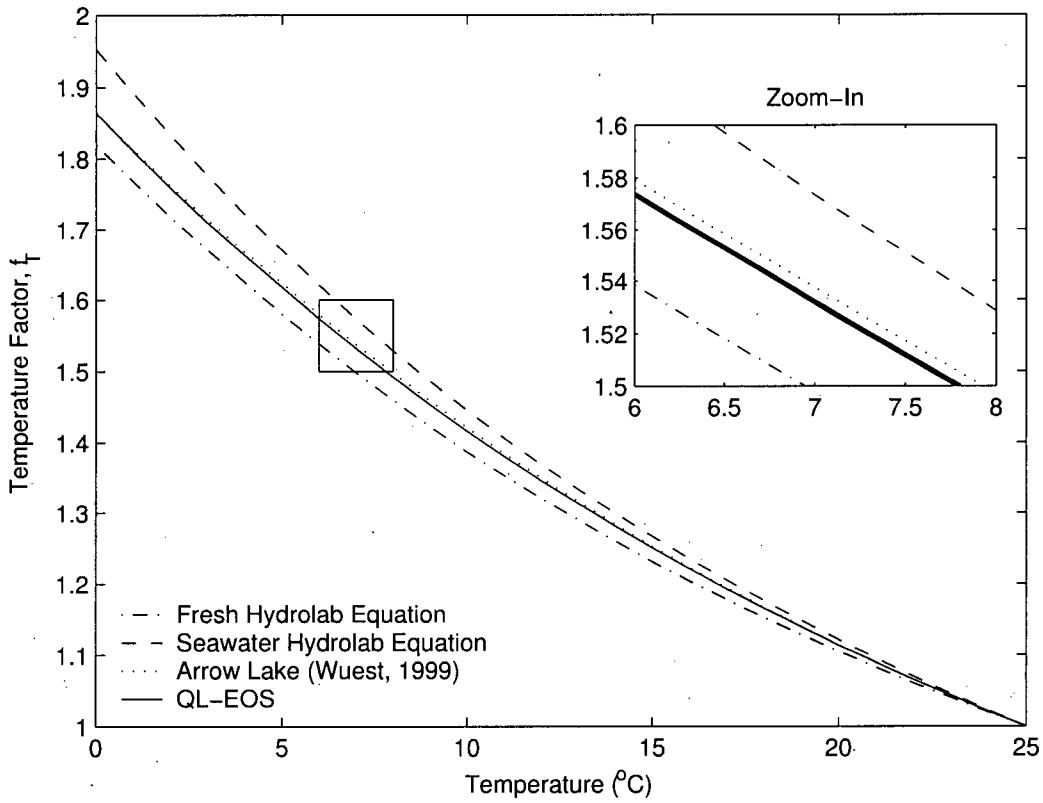

Figure 14: Temperature factor f_T function for Quesnel Lake compared to other f_T functions of interest.

The assumption that the conductivity readings reflect all dissolved solids (both ionic and non-ionic) is one source of error in the equation of state developed specifically for Quesnel Lake. This error will be assessed later in this section.

The relationship for the temperature factor, f_T, was determined according to the method described in Section 2.3.1:

$$f_T = 0.5369 + 0.0156 \cdot T + 1.339x10^{-4} \cdot T^2 - 7.552x10^{-7} \cdot T^3 \qquad (32)$$

Out of interest, this curve is compared to other curves generated for different lakes (Fig. 14). Notice the seawater and freshwater curves which bracket the Quesnel Lake

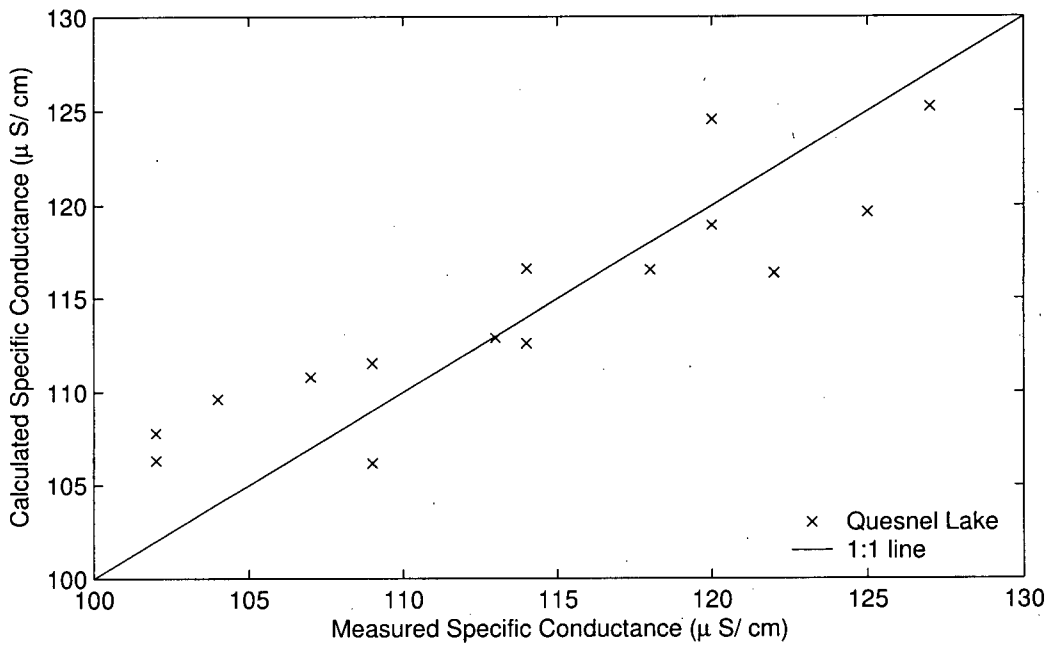

Figure 15: Measured and calculated specific conductance for 15 samples taken from Quesnel Lake July, 2003.

curve. Notice also that the Arrow Lake (which have a similar composition to Quesnel Lake) has a very similar f_T curve to Quesnel Lake.

To verify that the f_T curve for Quesnel Lake can accurately predict specific conductance values, calculated specific conductances are compared to specific conductance measured in the lab (Fig. 15). This data does not lie perfectly on the one to one line. However, the R^2 value for this data is $R^2 = 0.85$ indicating that more than 50% of the data is described by the 1 to 1 line. Error introduce by making this assumption will be discussed further in Section 4.3.3.

Quesnel Lake data were compared to calculated specific conductances from other B.C. lakes including Arrow Lake, Slocan Lake and Kootenay Lake, for comparison over a larger range of specific conductances (Fig. 16). The plot shows that the Quesnel Lake data falls in a cluster over a small range of specific conductance compared to the

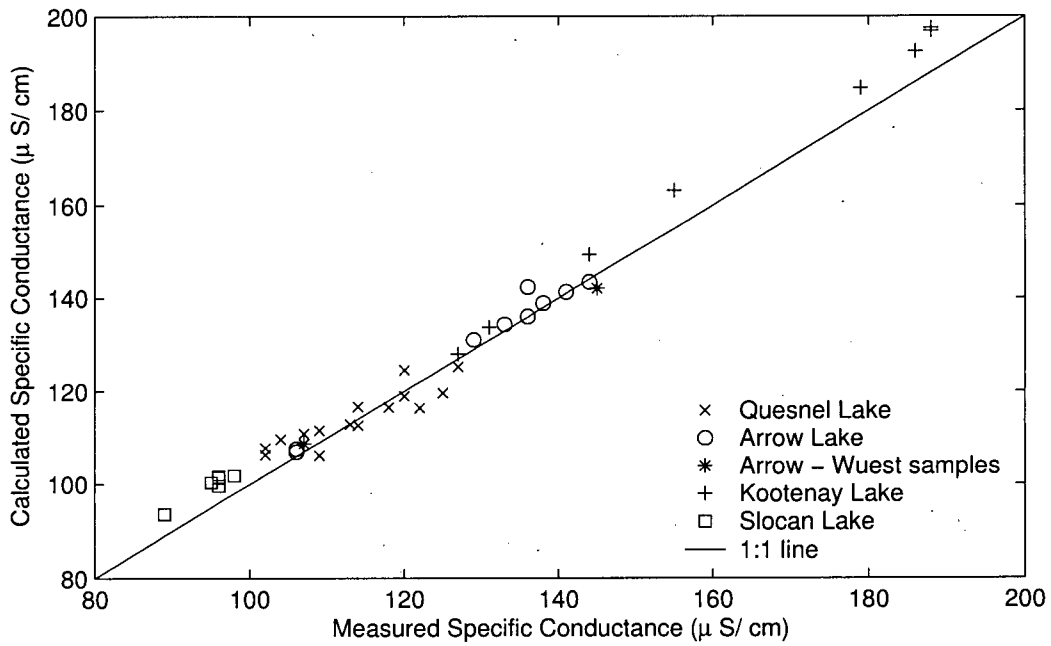

Figure 16: Comparison of Measured and Calculated Specific Conductance for Arrow, Slocan, Kootenay and Quesnel Lakes. Arrow, Slocan and Kootenay Lakes data courtesy Roger Pieters unless otherwise marked.

range of specific conductances found in nearby lakes. Although, Fig. 15 shows that the calculated specific conductances vary from the measured specific conductances, Fig. 16 suggests that this variability may be a symptom of the samples having been taken over a small range of salinity. Over a larger range of salinity, this variability appears less drastic. A further discussion of estimates of error can be found in Section 4.3.3.

4.2 Equation for Salinity

4.2.1 Finding the Constant of Proportionality, A

Salinity and measured specific conductance were plotted for all 15 samples collected from Quesnel Lake in July, 2003 (Fig. 17). A is the slope of the best fit line which

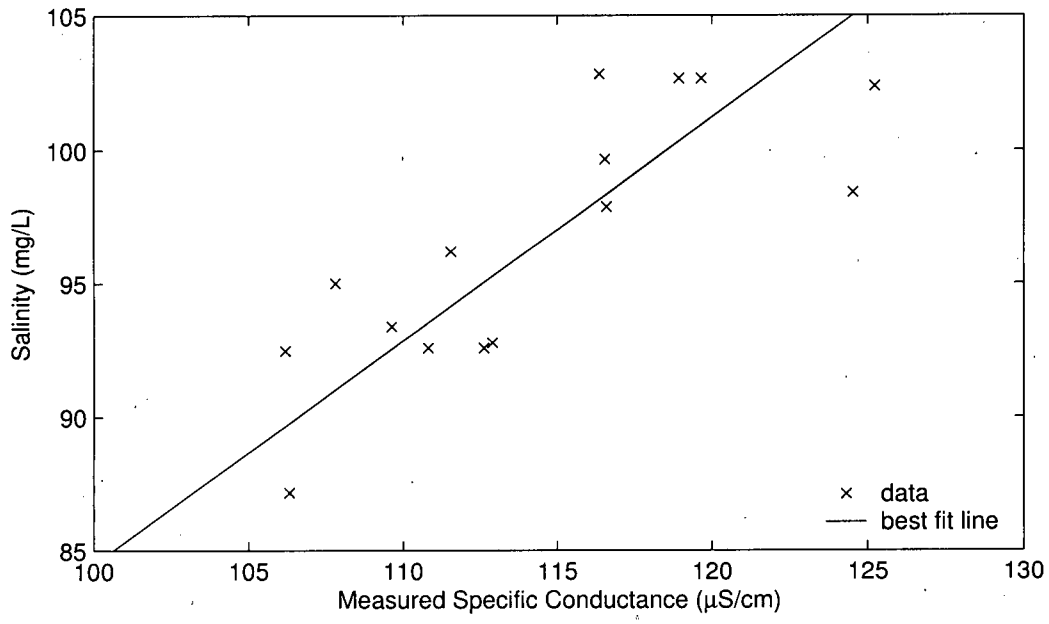

Figure 17: Measured specific conductance plotted as a function of salinity in order to determine the value for A for Quesnel Lake. Data from all 15 Quesnel Lake samples are plotted with a solid line showing the best fit value for A.

passes through the origin. The value of A was determined empirically to be:

$$A = 0.836mg \cdot cm \cdot L^{-1} \cdot \mu S^{-1} \tag{33}$$

Fig. 17 shows some variability in the value of A determined from individual samples. Again, this variability could cause error that will be discussed further in Section 4.3.3.

4.2.2 Salinity Equation

Eq. 3 can be substituted into Eq. 23 and rewritten as:

$$S_{CTD} = A \cdot \frac{C_T^P}{f_T \cdot f_P} \tag{34}$$

In this way, once A (Eq. 33) and the functional form of f_T (Eq. 32) are determined for a specific lake, the salinity can be found throughout the water column with CTD

measurements. This was done for the samples collected from Quesnel Lake in the summer of 2003 to give a lake specific expression for salinity:

$$S_{CTD} = \frac{0.836 \cdot C_T^P}{(0.5369 + 0.0156 \cdot T + 1.339x10^{-4} \cdot T^2 - 7.552x10^{-7} \cdot T^3) \cdot f_P(P,T)} \quad (35)$$

where the pressure function taken from Wuest et al. (1996) is given by:

$$f_P(P,T) = 1 + \gamma \cdot p \quad (36)$$

and

$$\gamma = 10^{-5} \cdot (1.856 - 0.05601 \cdot T + 0.0007 \cdot T^2) \quad (37)$$

In Eq. 35, C, T, and P are all measured with a CTD. After a relationship for salinity is determined in terms of easily measurable quantities, EOS_{QL} can be applied to calculate density as described in the next section.

4.3 Equation of State for Quesnel Lake

4.3.1 Coefficient of Haline Contraction

The analysis of the chemical constituents in Quesnel Lake water samples described in Section 3.4 predicts the value for the coefficient of haline contraction, β, to be:

$$\beta_{Quesnel} = 0.827mg \cdot L^{-1} \quad (38)$$

This Quesnel Lake specific coefficient of haline contraction can now be integrated into EOS_{CM} to obtain EOS_{QL}. To do this, the procedure described by Wuest et al. (1996) is used. $\beta_{Quesnel}$ is related to the Chen and Millero coefficient of haline contraction, $\beta_{Chen+Millero}$:

$$\beta_{Quesnel} = 1.096 \cdot \beta_{Chen+Millero} \quad (39)$$

and this new coefficient of haline contraction will be used to modify EOS_{CM} according to Eq. 40.

$$\rho_{Quesnel} = \rho_o(1 + 1.096 \cdot \beta_{Chen+Millero} \cdot S) \quad (40)$$

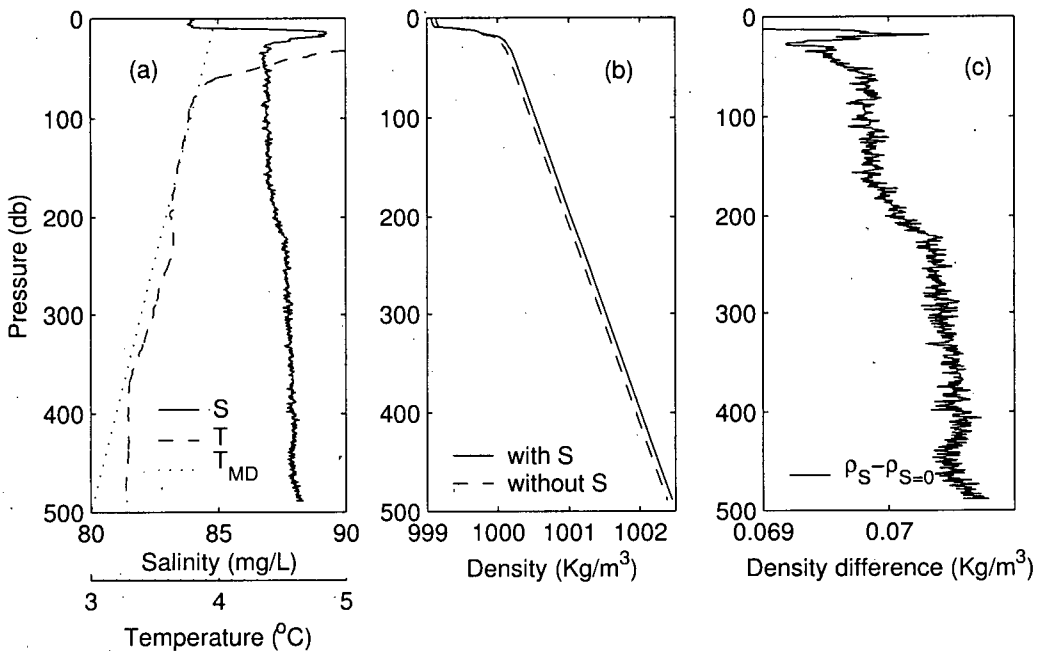

Figure 18: Comparing density with and without Quesnel Lake salinity contribution: (a) T and S profiles from the deep basin of Quesnel Lake, 2001. (b) Profiles of density, with and without the contribution from S. (c) Difference betwen density estimated using S calculated using Eq. 35 and density estimated with S=0.

Fig. 18a shows T and S profiles from the deep basin of Quesnel Lake. Below approximately 100m, the temperature roughly follows T_{MD}. At temperatures near T_{MD}, the thermal expansion coefficient is near-zero, and so small salinity effects play an important role in determining water column stability. To illustrate this, Fig. 18b shows the corresponding profiles of density, both with and without the contribution from salinity and Fig. 18c shows the difference between these two curves. This difference highlights the importance of salinity's contribution to density in understanding vertical mixing processes in the deep waters of Quesnel Lake.

4.3.2 Quesnel Lake's Equation of State

EOS_{CM} is modified for Quesnel Lake salinity according to Eq. 29 to produce EOS_{QL}:

$$\begin{aligned}\rho_{Quesnel} = 0.9998395 + 6.7914 \cdot 10^{-5} \cdot T - 9.0894 \cdot 10^{-6} \cdot T^2 \cdots \\ +1.0171 \cdot 10^{-7} \cdot T^3 - 1.2846 \cdot 10^{-9} \cdot T^4 \cdots \\ +1.592 \cdot 10^{-11} \cdot T^5 - 5.0125 \cdot 10^{-14} \cdot T^6 \cdots \\ +1.096 \cdot (8.181 \cdot 10^{-4} - 3.85 \cdot 10^{-6} \cdot T + 4.96 \cdot 10^{-8} \cdot T^2) \cdot S \end{aligned} \quad (41)$$

where S is determined from CTD data using a lake-specific equation (eq. 35).

4.3.3 Error

Fifteen samples taken throughout Quesnel Lake have been analysed to find f_T. Since this function is dependent on composition and since they have been taken from different parts of the lake, the question remains: to what accuracy can density be estimated from CTD data using a single equation of state?

Error is introduced into the developed EOS_{QL} by many avenues. They include the following:

- Error in the original measurements by PESC of concentrations of the major ions dissolved in Quesnel Lake;
- Error is introduced by using marine equations to find concentrations of components of the carbonate system for Quesnel Lake water;
- Error is introduced in the fitting process of polynomials to limiting equivalent conductivity and reduction coefficients data;
- EOS_{QL} has been found based on the composition of 15 samples taken from various places around Quesnel Lake, because some variability exists between these samples, EOS_{QL}, which is based on the average, will not be specific to different lake regions;

- Variability exists in the plot of Si vs. Ca (Fig. 13) showing that the assumption that they are regularly proportional is inaccurate, and;
- The charge balance for the average composition of the 15 samples is not zero, which may have an impact on the coefficient of haline contraction, β, determined in EOS_{QL}.

To assess error in EOS_{QL}, calculated densities were compared to densities measured directly with an Antor Paar densitometer. To calibrate the densitometer, the density of DDW was measured. Table 5 shows the expected and measured results of these measurements. Based on the root mean square of the differences between the expected and measured values, an offset of 2.6 x 10^{-6} g/cm^3 was assumed in subsequent density measurements.

Table 5: Measured Density values of distilled, deionized water (DDW) used to calibrate the Anton Paar Densitometer

Density of DDW	
Expected g/cm^3	Measured g/cm^3
0.998203	0.998204
	0.998205
	0.998205
	0.998206
	0.998207

The results of density measurements of all Quesnel Lake water samples collected in July 2003 and June 2004 are shown in Figures 19 and 20.

Fig. 19 shows measured densities and densities calculated with EOS_{QL} along with a 1:1 line. The outlier in the upper right hand corner of the plot was taken at the Niagara Creek inflow to Quesnel Lake's East Arm. This water had high silt content at the time of collection which may account for its uncharacteristically high specific conductivity. The linear correlation coefficient of the data in Fig. 19, excluding

the outlier, is $R^2 = 0.929$ indicating that 93% of the variation in density can be explained with the 1:1 line. This correlation coefficient is close to 1 suggesting a linear relationship between measured and calculated densities.

Also, to assess the need of developing a lake specific equation of state, densities calculated EOS_{CM} were compared to densities calculated with EOS_{QL} and densities measured with the densitometer (Fig. 20). Although the densities calculated using EOS_{QL} are often on the low end of the measured values, they are within the estimated error of the measured values. Also, the density values calculated with EOS_{QL} are closer to the measured valued than those calculated with EOS_{CM}. The standard deviation between measured values of density and those calculated with EOS_{QL} is 0.0018 kg/m^3. The standard deviation between measured values of density and those calculated with EOS_{CM} is 0.0157 kg/m^3 which is signficantly larger than that calculated with EOS_{QL}. EOS_{CM} describes Quesnel Lake water density less accurately than reported by Chen and Millero (1986). The outlier samples (samples 7 and 8 in Fig. 20) are again apparent. Neither EOS_{QL} nor EOS_{CM} accurately predict density for water in that area of the lake.

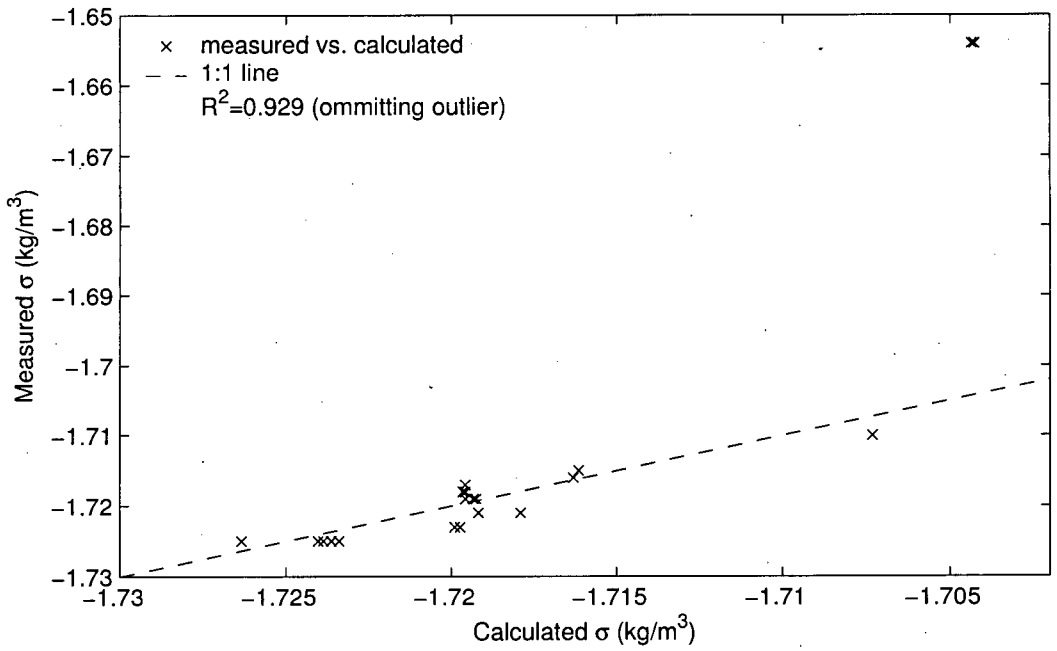

Figure 19: Measured and calculated densities for water samples collected from Quesnel Lake in July 2003 and June 2004. The outlier in the upper right hand corner of the plot was taken at the Niagara Creek inflow to Quesnel Lake's East Arm.

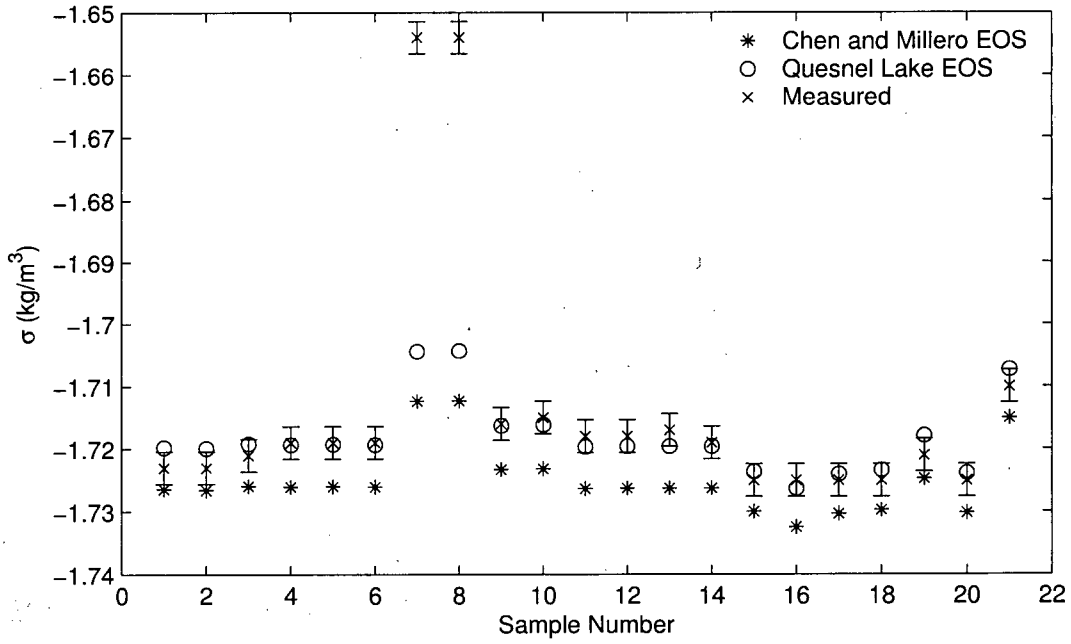

Figure 20: Comparison of densities at T=20 °C and P=0 bar in Quesnel Lake: density measured directly with the Anton Paar densitometer; density calculated with EOS_{QL}, and density calculated with EOS_{CM}. The outlier samples (samples 7 and 8) were taken at Niagara Creek inflow to Quesnel Lake's East Arm. Neither EOS_{QL} nor EOS_{CM} accurately predict density for water in that area of the lake.

5 Local Stability

Developing EOS_{QL} was done in the interest of investigating the deep water ventilation in Quesnel Lake. A preliminary look at vertical mixing gives an indication of where and how this ventilation is taking place. For this reason, profiles of quasi-density and the Brünt-Väisäla frequency have been found based on CTD profiles.

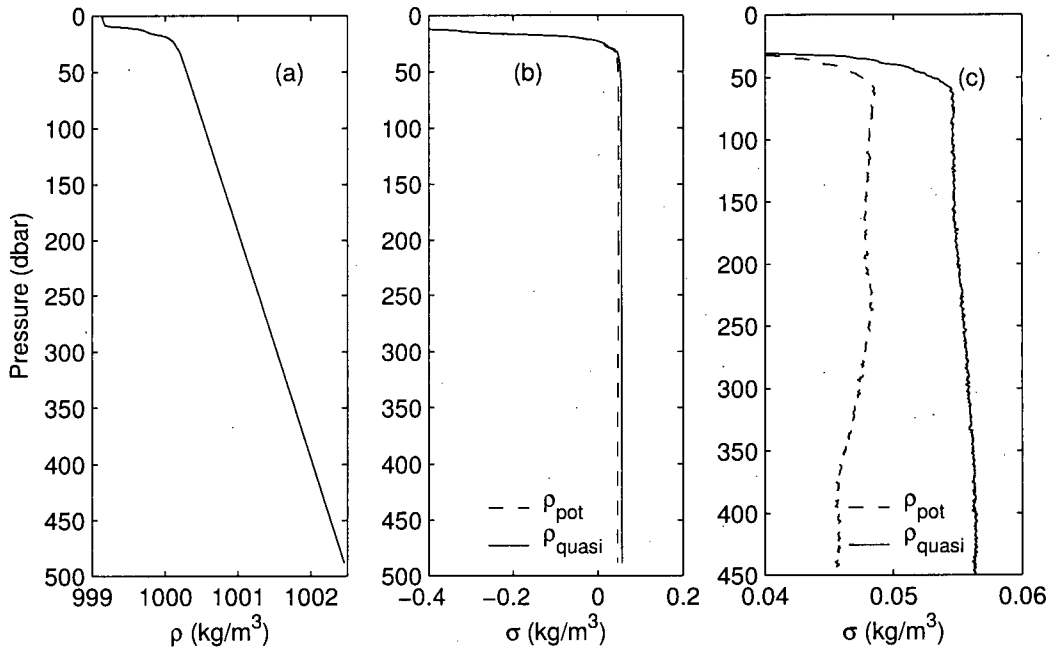

Figure 21: A comparison of potential and quasi densities for CTD profile taken in 2001: a) plot of in-situ density, b) potential and quasi-density, c) zoom-in of potential and quasi-density.

5.1 Quasi-Density

Quasi-density profiles were found according the procedure explained in Section 3.7.1. Fig. 21 illustrates the importance of using quasi-density for investigating local stability. Fig. 21a shows a plot of in-situ density. The hydrostatic pressure is the dominant

signal in this density plot. In order to get a plot of a quantity that can be used to assess column stability and compare densities from within a profile, this pressure signal must be removed. Both potential and quasi-density serve this purpose and plots of both for a CTD cast taken in the East Arm in 2001 are shown in Fig. 21b. Both of these return a virtually vertical profile - one with no hydrostatic pressure signal. Once zoomed in (Fig. 21c), one can see that the potential and quasi-density plots are not perfectly vertical. The potential density plot shows that below the thermocline, density gradually decreases thereby predicting a mostly unstable profile. Quasi-density predicts a profile which contains some instability but has nearly monotonically increasing densities and is stable. Quasi-density was shown to be more appropriate than potential density by arguments made in Section 2.4.2 and is supported by the validity of the pressure-free profiles predicted by each. In Quesnel Lake, quasi-density should be used to study local stability rather than potential density.

Quasi-density was found from a CTD profile using EOS_{QL} and EOS_{CM} to calculate in-situ density. Fig.22 shows this comparison. Quasi-density calculated with EOS_{QL} is different than that calculated with EOS_{CM}. However, the difference is primarily a simple offset in values; the structure of the profiles are still very similar. This will be explored further in Section 5.3 where the Brünt Väisäla Frequency is discussed.

Fig. 23 displays quasi-density profiles from the CTD data collected in the East Arm over three years (2001, 2002 and 2003) in order to gain insight into how the vertical structure in the water column varies over a period of time. Quasi-density profiles in the East Arm over the three year period all demonstrate very similar characteristics. Profiles have generally increasing slopes with density fluctuations of simlar magnitude.

Fig. 24 displays quasi-density profiles from the CTD data collected in July 2003 at each of the stations presented in Fig. 9 as well at the junction in order to gain insight on how vertical structure varies spatially throughout the lake. Quasi-density profiles from 2003, taken around Quesnel Lake, show different characteristics. The profile taken at the junction echoes characteristics of profiles taken in the North and

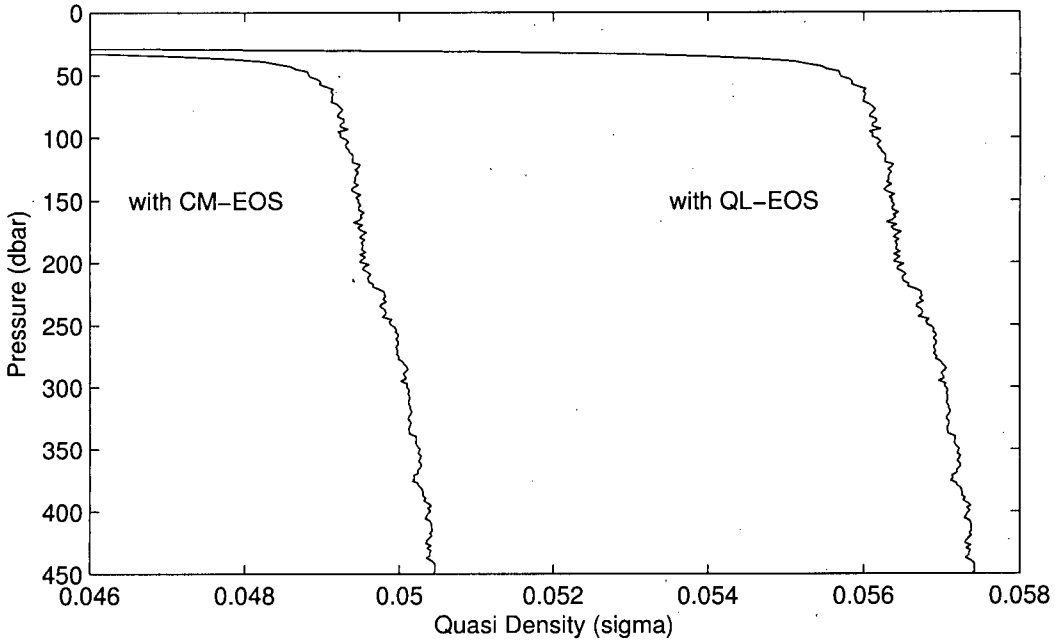

Figure 22: EOS_{CM} and EOS_{QL} for CTD profile taken in 2001. Although density values are different, the water column stability is roughly the same in each profile.

West Arms. For example, three small spikes in the West Arm profile at 65, 145 and 200 dbar are also present in the Junction profile at the same depths. A small step in quasi-density at 105 dbar in the North Arm is also present in the Junction profile at the same depth.

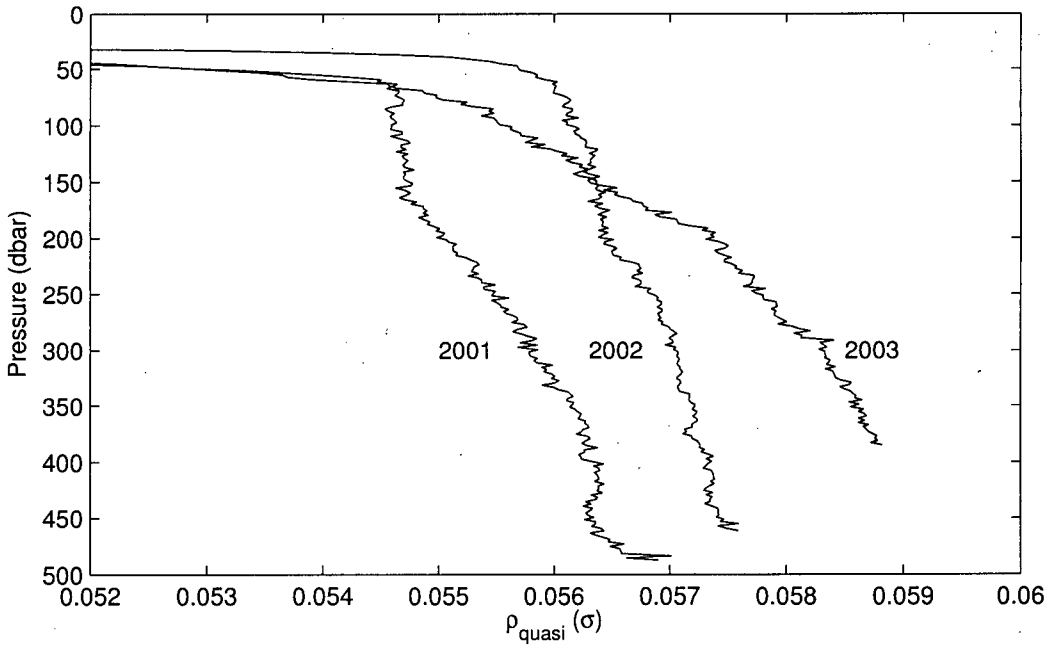

Figure 23: Quasi-density profiles for 2001, 2002, and 2003.

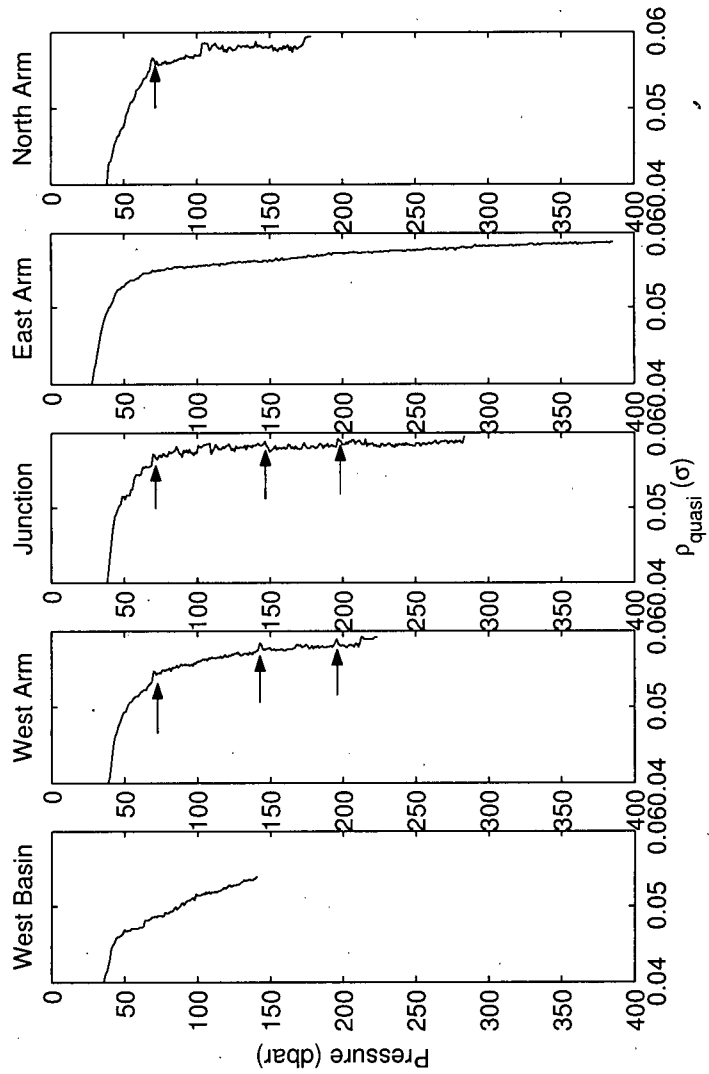

Figure 24: Quasi-density profiles based on CTD profiles taken in 2003 at stations in the East Arm, North Arm, Junction, West Arm, and West Basin.

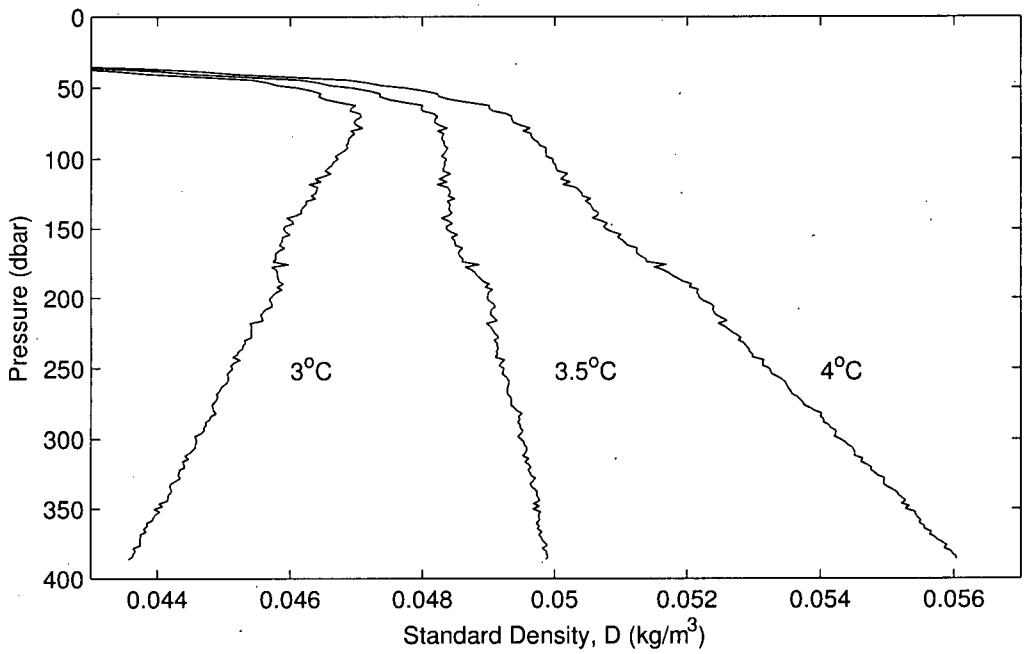

Figure 25: Standard density calculated by varying the temperature, T_o, of the reference parcel to temperatures bracketing T_{MD} in Quesnel Lake (3°C to 4°C).

5.2 Standard Density

The value calculated for standard density is very sensitive to which temperature is chosen as the temperature of the reference parcel and less sensitive to the reference parcel's salinity. Fig. 25 shows the standard density profiles calculated for the CTD cast collected at Quesnel Lake in 2001 with varying temperatures which bracket the variation in deep temepratures in Quesnel Lake chosen as the reference.

Fig. 25 illustrates that the choice of reference temperature is critical to calculating a quantity that is meaningful for finding local stability in the water column. Standard density calculated from the 2001 Quesnel Lake CTD casts with $T_o = 3°C$ shows an almost entirely unstable profile while the same CTD cast calculated with $T_o = 4°C$ shows an almost entirely stable profile.

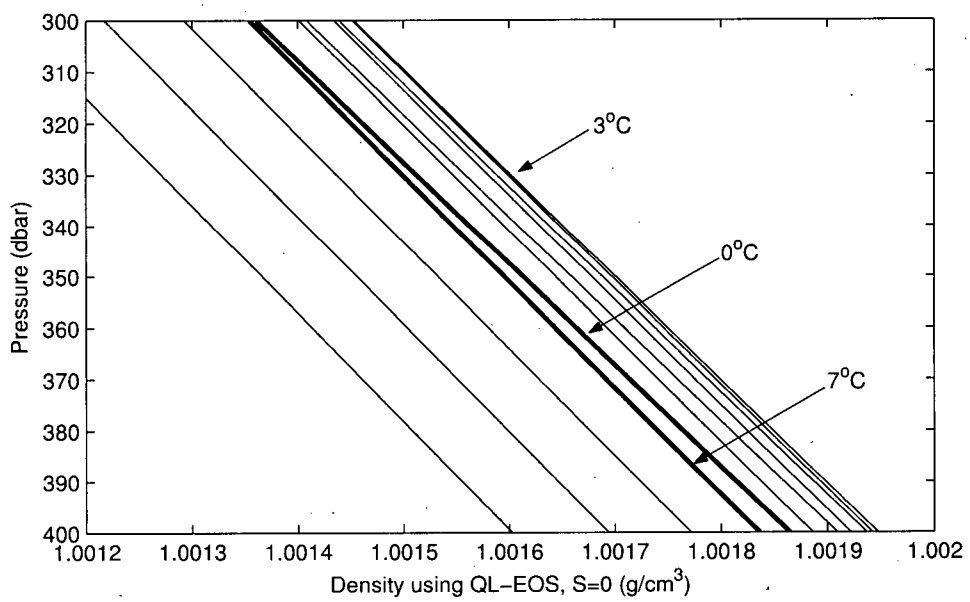

Figure 26: Density as a function of Temperature and Pressure (2D). The inset shows a blow up of the indicated region with bolded line illustrating the difference in slope between density gradients at 0°C and 7°C.

The reason for this difference lies in the assumption that the change in density due to pressure at one temperature is equal to the change in density due to pressure at another temperature. Figures 26 helps to illustrate this point. Fig. 26 is a plot of density as a function of pressure with multiple lines showing this dependence for varying temperatures. The bold lines highlight the density gradients at two temperatures, one higher than T_{MD} at 7°C, and one lower at 0°C. These lines are not parallel. The gradients of density with pressure are different at adjacent temperatures. This make it inappropriate to try to predict the change in density with pressure based on a parcel at a reference temperature different than the in-situ temperature with water neat T_{MD}.

Significant error would be introduced if standard density were calculated for a profile near 0°C with a reference parcel assumed to be at 7°C. This example illus-

trates an extreme case and gradients do become more similar at closer temperatures. However, this difference in gradients is large enough near T_{MD} to cause errors when using standard density to assess stability.

Standard density performed well for the work Foster (1995) did in the Antarctic. He suggests that standard density is only valid for small temperature ranges. More accurately, standard density is only valid for small ranges of temperature away from T_{MD} where the changes of density with pressure are more uniform for neighbouring temperatures. Because Foster (1995) is applying the standard density concept in salt water, water that will freeze before approaching its temperature of maximum density, the anomalies which occur near T_{MD} in fresh water are inconsequential to his work. However, standard density cannot be applied to the investigation of deep water ventilation of Quesnel Lake water, whose water temperature mostly lies near T_{MD}.

5.3 Instability Identification

Quasi-density is used to calculate the Brünt Väisäla frequency in order to identify where density inversions occur. Quasi-density is noisy when calculated directly from CTD profiler data. Consequently, the Brünt Väisäla frequency calculated from quasi-density is also noisy — too noisy to identify instabilities. To filter out noise and to gain a meaningful signal, the quasi-density profile is smoothed through bin averaging. The total change in density over the instability is less than the fluctuations in unfiltered quasi-density, illustrating the need to bin average. By identifying the trends in the quasi-density data over a resolution of interest, instabilities of that resolution size are identified. Fig. 27 shows a blown up section of the quasi-density profile with an inset of the entire profile. The blown up section of the profile also features the profile after bin averaging has been performed with various bin sizes.

A power spectrum for this quasi-density profile is shown in Fig. 28 on a log-log scale. Because so many frequencies are present in the quasi-density profile in Fig. 27, the power spectrum plot was generated in order to determine if there is some obvious

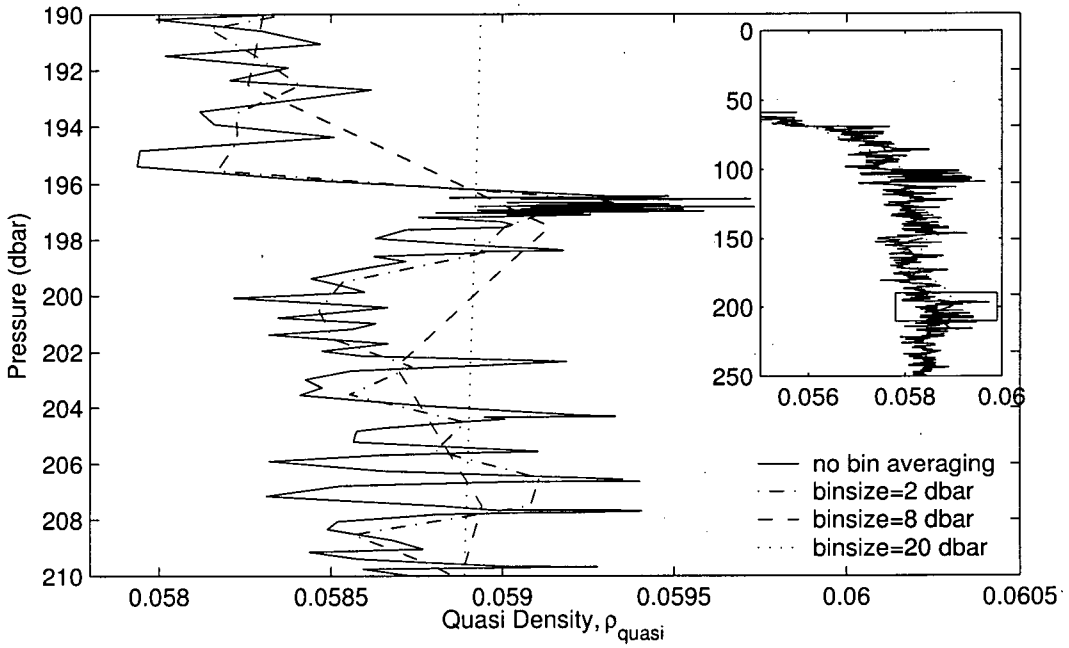

Figure 27: Quasi-density of CTD profile taken in 2003 in Quesnel Lake's Junction bin averaged to remove noise from signal into bin of sizes 2 dbar, 8 dbar and 20 dbar. The insert shows the entire profile.

feature that could impartially help select a cutoff frequency for which signals with greater frequency could be considered noise. Fig. 28 displays frequency power data with a relatively constant negative slope and no such feature is present.

Brünt Väisäla frequency plots are examined with various frequencies filtered out using bin averaging. The Brünt Väisäla frequency, N^2, and its error have been found for three bin sizes: 2, 8 and 20 dbar (Fig. 29). The N^2 profiles where found using EOS_{QL}. For progressively smaller bin sizes N^2 becomes less noisy and its error also becomes smaller. The mean error in N^2 for profiles found with bin sizes 2 dbar, 8 dbar and 20 dbar are 5.5 x 10^{-7} s^{-2}, 1.6 x 10^{-7} s^{-2}, and 7.4 x 10^{-8} s^{-2} respectively (see Section 3.7.3) . However, vertical resolution is lost in this process. It is crucial to know what size instability is of interest to know what size bin to choose. Choosing

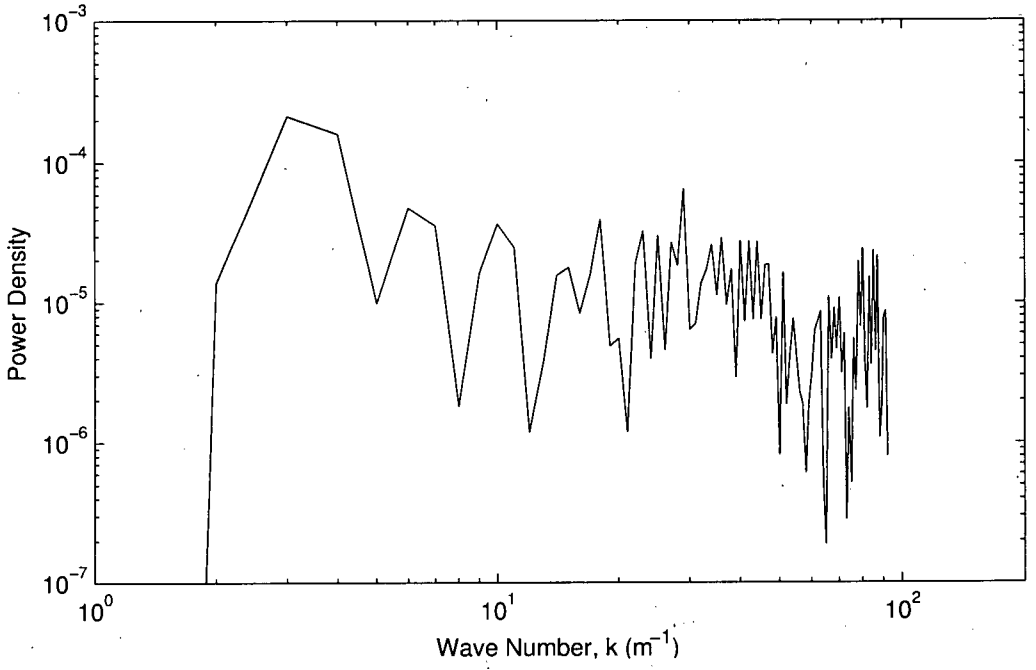

Figure 28: Power Spectrum for the unfiltered quasi-density profile taken in 2003 at the Junction in Quesnel Lake.

too large a bin may reduce resolution to a point where instabilities of interest are no longer visible as was done for this profile with a bin size of 20 dbar. For the purpose of this study, a bin size of 8 dbar was used to compare N^2 profiles calculated from CTD profiles taken in Quesnel Lake's East Arm in 2001, 2002, and 2003. Also, N^2 profiles taken in 2003 from Quesnel Lake's three Arms, Junction and West Basin are also compared.

From this series of profiles, one is able to deduce the resolution at which water column is completely stable. For example, the centre plot in Fig. 29 shows that when looking at a resolution of 8 dbar, there are some places in the profile that are slightly unstable. However, at a resolution of 20 dbar, the entire water column appears to be neutrally stable.

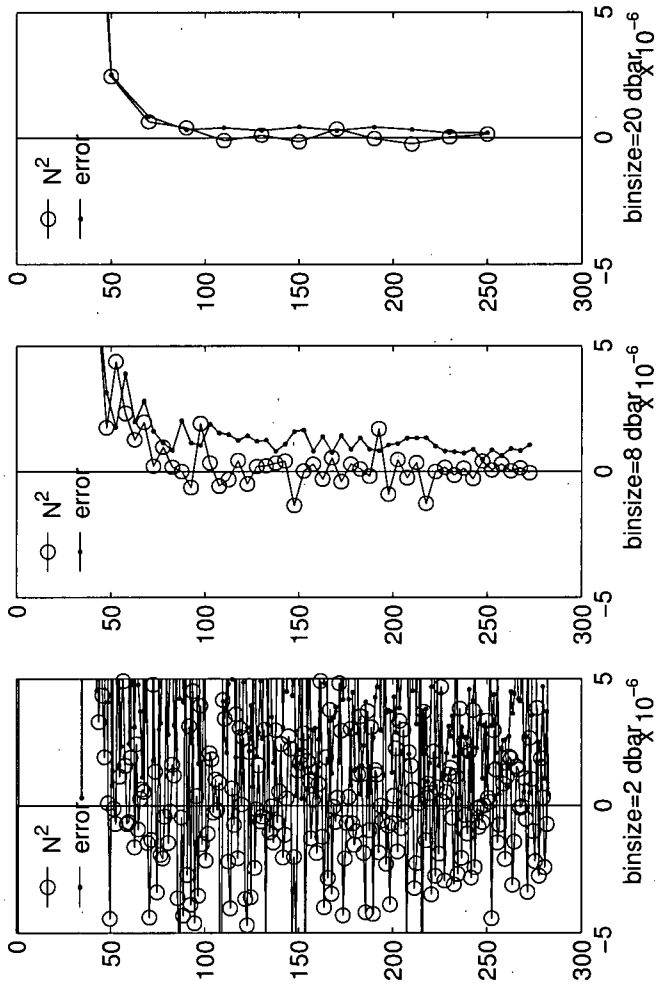

Figure 29: Brünt Väisäla frequency of CTD profile taken in 2003 in Quesnel Lake's Junction found using Quasi-density averaged in to bins of sizes 2 dbar, 8 dbar and 20 dbar. The error in the Brünt Väisäla frequency is also plotted for each of these bin sizes.

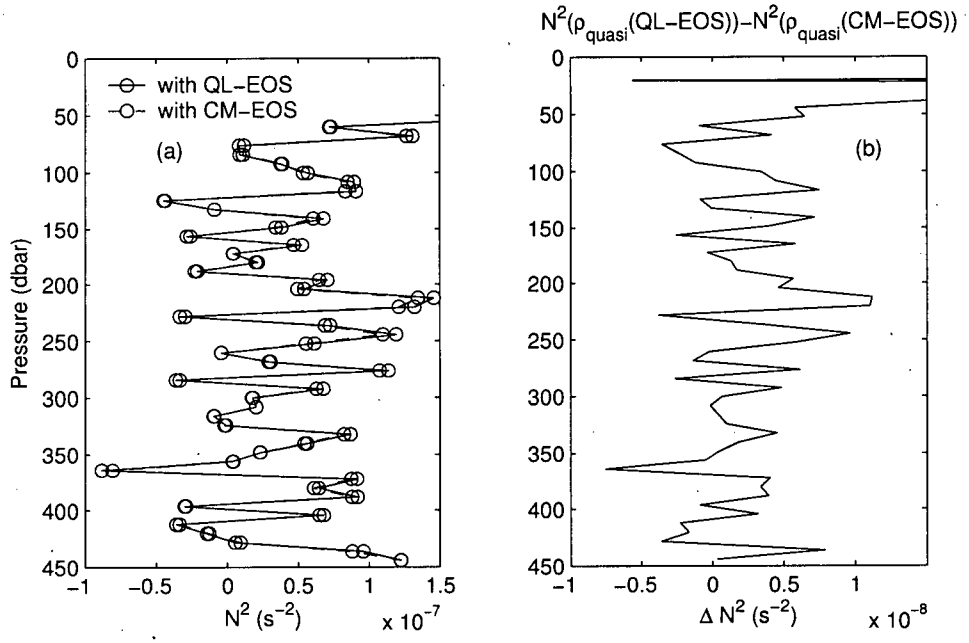

Figure 30: a)Brünt Väisäla Frequency found using EOS_{CM} and EOS_{QL} for CTD profile taken in 2001, b) the difference between N^2 calculated with $\rho_{quasi}(\mathrm{EOS}_{QL})$ and $\rho_{quasi}(\mathrm{EOS}_{CM})$.

Fig. 30 shows N^2 calculated for the profile taken in 2001 (for comparison with profiles featured in Fig. 22) with quasi-density using both EOS_{QL} and EOS_{CM} for comparison as well as the difference in the two quantities. The two equations of state predict very similar profiles. The difference indicates that EOS_{QL} shows greater stratification through the water column and so estimates that instabilities are more unstable and that stabilities are more stable than what EOS_{CM} estimates. However, the structure (i.e. gradient) predicted by the two equations of state are nearly indistinguishable.

Fig. 31 shows N^2 calculated with both potential and quasi-density for comparison based on densities calculated with EOS_{QL}. In Fig. 21, potential density portrays a profile with an unstable region (i.e. positive slope) below approximately 250 m. This is echoed in N^2 profile of the potential density profile.

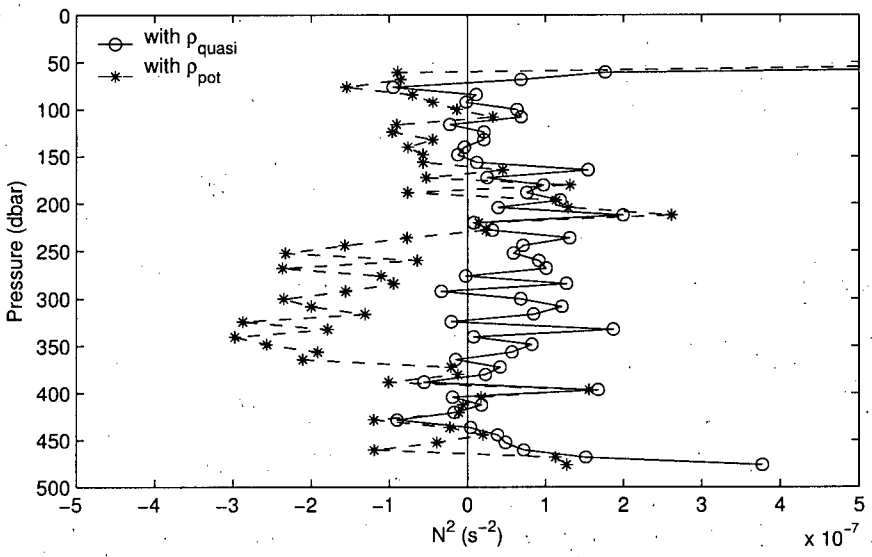

Figure 31: Brünt Väisäla Frequency found using $\rho_{potential}$ and ρ_{quasi} for CTD profile taken in 2001.

Fig. 32 displays N^2 profiles from the CTD data collected in the East Arm over three years (2001, 2002 and 2003) in order to gain some perspective how the vertical structure in the water column varies over a period of time. Fig. 33 displays N^2 profiles from the CTD data collected at each of the stations presented in Fig. 9 as well at the junction in order to gain some perspective on how vertical structure varies spatially throughout the lake. Again, N^2 profiles in the East Arm over the three year period all demonstrate very similar characteristics. Profiles indicate that the majority of the water column below approximately 50 m is close to being neutrally stable, save some locations in 2001 and 2002 where the profile becomes slightly unstable. N^2 profiles from 2001 and 2002 both exhibit these unstable regions near 400m depth.

Quasi-density profiles taken in 2003, from the different areas around Quesnel Lake, show differing characteristics. The East Arm profile has $N^2 \sim 0$ s^{-2} below 50 m. Compared to other areas in Quesnel Lake, the East Arm is relatively neutrally stable. This may be an indicator as to how deep water ventilation is taking place in this region of the lake.

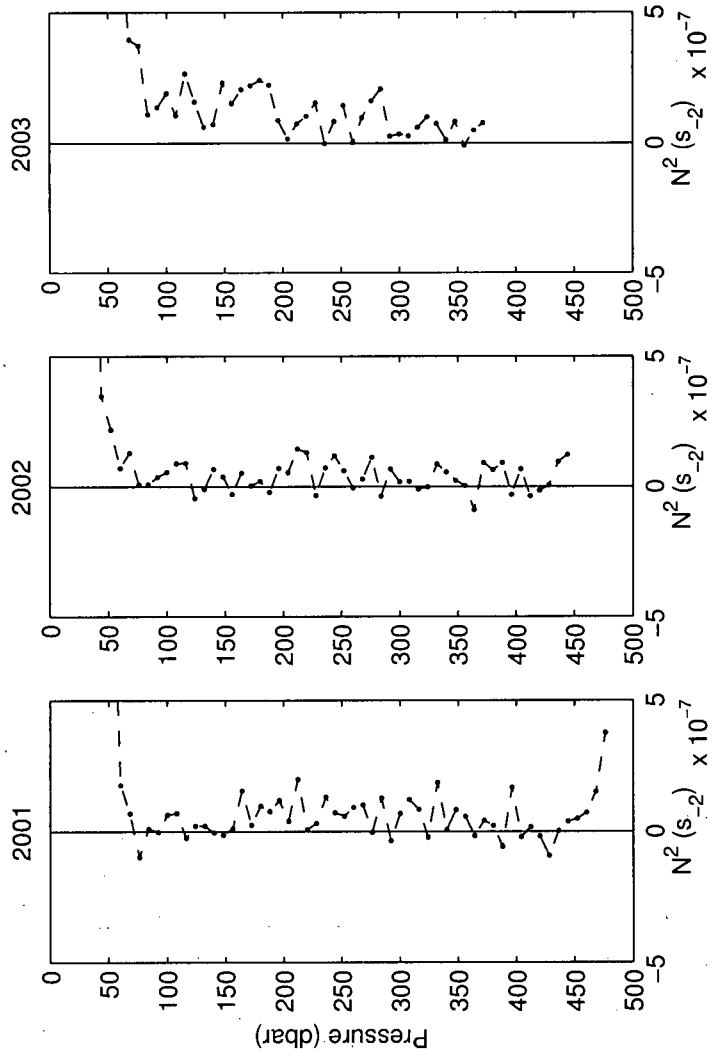

Figure 32: Profiles of the Brünt Väisäla Frequency based on CTD profiles taken in 2001, 2002, and 2003 bin-averaged to 8 dbar.

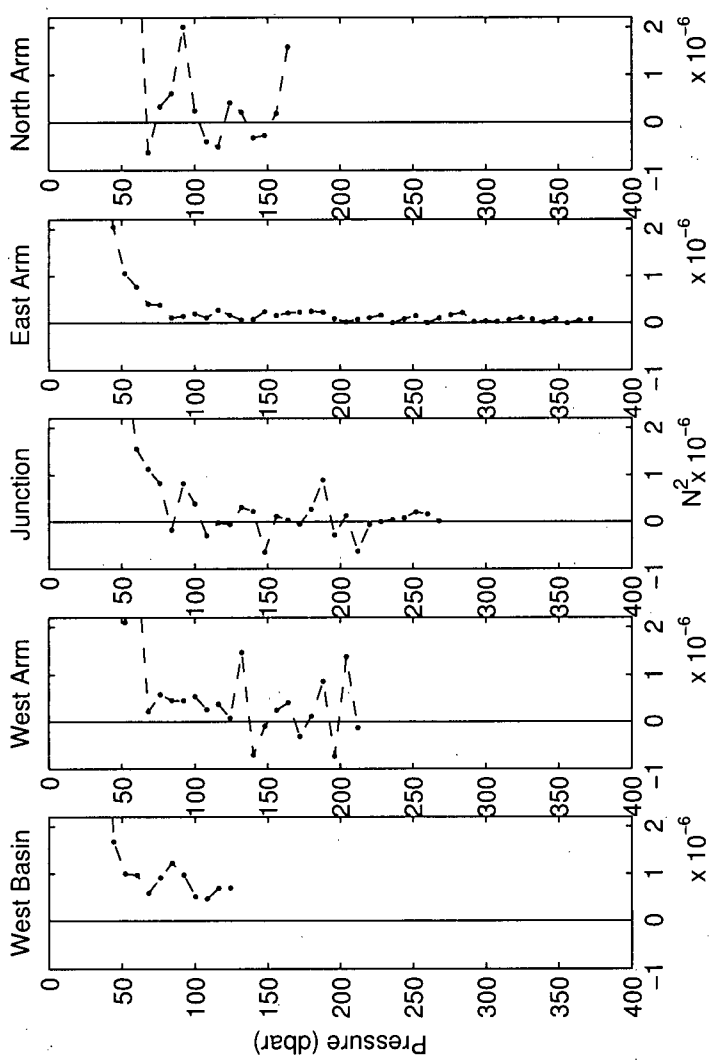

Figure 33: Profiles of the Brünt Väisäla Frequency based on CTD profiles taken in 2003 at stations in the East Arm, North Arm, Junction, West Arm, and West Basin bin-averaged to 8 dbar.

5.4 Density Currents

The formation of a density current at the mouth of the Niagara Creek is one mechnism that could contribute to the deep water ventilation in Quesnel Lake. Niagara Creek water originates in a glaciated catchment and is heavily loaded with silt. This silt may increase the density of incoming river water enough to overcome the barrier caused by the temperature of maximum density previously described.

To illustrate the mechanism, Fig. 34 shows a schematic of the density current. In Fig. 34a, where incoming riverine water is near the deep (P $\approx$ 500 dbar) T_{MD} (2.93 ^{o}C), cold, silt loaded river water passes through surface waters (which, in the absence of silt, would be lighter than water at the surface T_{MD}), and, via the density current, is driven to the bottom of the lake. Entrainment of the surrounding water would increase the volume of the density current as it plunges. This, together with the gradually smaller density difference between the density current and its surroundings as the denisty current reaches greater depths, would cause the density current to lose momentum. The density current water could potentially reach the lake bottom and ventilate Quesnel Lake's deep water.

In Fig. 34b, where incoming riverine water is near the surface T_{MD}, river water is again driven to the lake bottom via the density current, but as the water loses momentum, silt will settle out of the river water. The clarified river water then becomes buoyant and begins to move upward to a depth where the it has the same temperature as the surrounding water's T_{MD} and is neutrally stable. In the latter case, bottom water will be entrained and the mixed river/lake water will move upward together contributing to the flux of nutrients to the surface.

Due to seasonal variation in river temperature and flow, which entrains varying amounts of silt, the density difference between incoming river water and lake water will vary. Because of this variation in the density current's density, as it loses momentum, varying degrees of silt will be unloaded before the water becomes buoyant. Together, these factors lead to cases where the process described above is modified. Above, two

idealised cases are described, whereas in reality, Niagara Creek plunges to varying depth, and surfaces with varying clarity. The re-surfacing density current waters, which have been cycled up from deep parts of the lake, will be cold and have some suspended particulates.

Evidence for the density driven mechanism comes from direct density measurements on samples collected from Niagara Creek on June 23, 2004. These density measurements show that Niagara Creek water density is significanly larger than rest of lake. At atmospheric pressure and a temperature of 20.000 $\pm$ 0.001 ^{o}C, $\rho_{Niagara} = 998.3480 \pm 0.0026 kg/m^3$ and $\rho_{Quesnel} = 998.2818 \pm 0.0026 kg/m^3$. Niagara Creek water would remain denser than Quesnel Lake water through mechanical compression as it plunges. Samples 7 and 8 in Fig. 20 were collected within the turbid plume at the Niagara Creek inflow. Samples 9 and 10 were collected just outside of that plume. Density calculated using on EOS_{CM} and EOS_{QL} based on water sample conductivity and temperature greatly underestimate the measured density. The measured density includes the density from non-ionic constituents in the sample water which contribute significantly in Niagara Creek water density. This additional non-ionic material is likely the silt mentioned above.

The N^2 profiles found for the East Arm in 2001, 2002, and 2003 (Fig. 32) indicate that the whole water column is close to neutrally stable. This may result from the homogenizing effect the plume generates as the density current loses silt and convects upwards to its depth of neutral stability. Density current water then remains at a depth where it is neutrally buoyant until it experiences any subsequent external forcing.

Indirect evidence also supports this mechanism. Visual observations suggest that water in the East Arm has lower transparency compared to the rest of the lake (personal communication from Daniel Potts, June, 2004; also observed by Christina James in July 2003, and September 2004). This is likely due to unsettled silt moved to the surface by the buoyant density current water.

Note, the surface water in the East Arm was found to be colder than surface

temperatures in the rest of the lake in the summer months in two studies. In the fall of 1981, surface temperatures in the lake's East Arm were 4.5 °C colder than the West Basin (Stockner and Costella, 1980). In 1982, surface temperatures in the East Arm were again observed to be colder than the junction by 8.5 °C in June and by 4.5 °C in August (Morton and Williams, 1990).

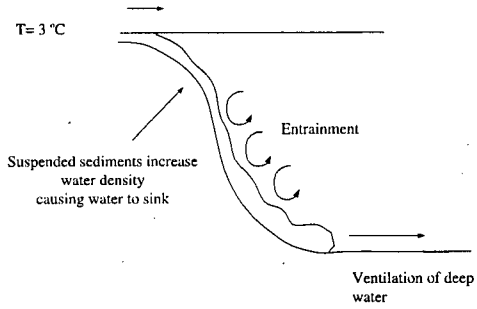

(a)

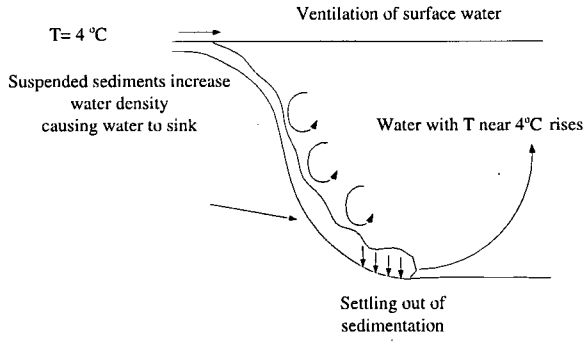

(b)

Figure 34: Illustration of density current: (a) water with $T \simeq 3°C$ sinks through surface water due to addition of suspended sediments (b) water with $T \simeq 4°C$ sinks through bottom water due to sediment load and, after sediments settle out, water rises to surface.

6 Conclusion

Deep water ventilation in Quesnel Lake, which controls the oxygenation of deep water and recycling of nutrients to surface waters, is of importance to fish within the lake and impacts the salmon population in the Fraser River. The objective of this research was to develop an accurate equation of state for Quesnel Lake for use with CTD profiler data in order to be able to investigate deep water ventilation.

Water samples and CTD profiles were collected in July 2003. Water samples were analysed for concentrations of constituents, pH, alkalinity and specific conductance. From these quantities, an equation relating in-situ salinity to CTD parameters was developed:

$$S_{CTD} = \frac{0.836 \cdot C_T^P}{(0.5369 + 0.0156 \cdot T + 1.339x10^{-4} \cdot T^2 - 7.552x10^{-7} \cdot T^3) \cdot f_P(P,T)}$$

where the pressure function taken from Wuest et al. (1996) is given by:

$$f_P(P,T) = 1 + \gamma \cdot p$$

and

$$\gamma = 10^{-5} \cdot (1.856 - 0.05601[dbar^{-1o}C^{-1}] \cdot T + 0.0007[dbar^{-1o}C^{-2}] \cdot T^2)$$

The coefficient of haline contraction was determined to be $\beta_{Quesnel} = 0.827$ mg/L^{-1} or $\beta_{Quesnel} = 1.096 \cdot \beta_{Chen+Millero}$ for the composition of Quesnel Lake. The coefficient of haline contraction was used to modify the equation of state developed for waters in the limnological range by Chen and Millero (1986) as follows:

$$\begin{aligned} \rho_{Quesnel} = 0.9998395 + 6.7914 \cdot 10^{-5} \cdot T - 9.0894 \cdot 10^{-6} \cdot T^2 \cdots \\ +1.0171 \cdot 10^{-7} \cdot T^3 - 1.2846 \cdot 10^{-9} \cdot T^4 \cdots \\ +1.592 \cdot 10^{-11} \cdot T^5 - 5.0125 \cdot 10^{-14} \cdot T^6 \cdots \\ +1.096 \cdot (8.181 \cdot 10^{-4} - 3.85 \cdot 10^{-6} \cdot T + 4.96 \cdot 10^{-8} \cdot T^2) \cdot S \end{aligned}$$

where S is determined from CTD data using the above lake-specific equation.

Based on the values shown in Fig. 20, one can conclude that EOS_{QL} accurately estimates density for Quesnel Lake to within 0.0018 kg/m^3; significantly better than the alternative, EOS_{CM}, which is accurate to 0.0158 kg/m^3.

The equation of state was developed in order to obtain accurate estimates of density to investigate vertical stability in a water column. Generally, when investigating vertical stability, potential density is used to remove the hydrostatic compressibility in order to compare water parcel densities within a profile. Also, standard density has been used for similar reasons. However, neither standard density nor potential density can be applied to the investigation of deep water ventilation of Quesnel Lake, where water temperature lies near T_{MD}. Quasi-density profiles show generally increasing density through the water that provide a more likely representation of stability than either potential or standard density profiles. In Quesnel Lake, and other deep temperate lakes, quasi-density should be used to study local stability.

Quasi-density profiles were generated from CTD data in the East Arm from 2001, 2002 and 2003 as well as the North Arm, West Arm, West Basin and Junction for 2003. East Arm profiles from all three years show very smooth quasi-density profiles. In 2003, features present in quasi-density profiles from the North Arm and West Arm are echoed in the profile from the Junction.

Quasi-density profiles were used to compute profiles of the Brünt Väisäla frequency, N^2, which identify where instabilities occur within the water column. To find N^2, ρ_{quasi} data should filtered by bin-averaging using a bin size that is appropriate for the size of density inversion that is of interest. N^2 profiles calculated with EOS_{QL} and EOS_{CM} were compared. There was not a significant difference in the stability predicted by each. N^2 profiles calculated with potential density and quasi-density were also compared. Potential density predicted a mostly unstable profile while quasi-desnity predicted a more stable and, therefore, more realistic profile.

Brünt Väisäla frequency profiles indicate that the water column in Quesnel Lake's East Arm is close to neutrally stable in the three years in this study, with weak instabilities occurring near 400m depth. However, Brünt Väisäla frequency profiles

for the other areas in the lake in 2003 show larger regions of instability between 50m and 200m depth indicating that mixing may be taking place in those areas.

Brünt Väisäla frequency profiles showing neutral stability in Quesnel Lake's East Arm is evidence of a density current contributing to deep water ventilation. The limited transparency, as well as cooler surface temperatures through the summer months also support this theory.

7 Future Work

The natural progression of the research carried out on Quesnel Lake in future will include determining a Thorpe Scale for overturns identified in CTD profiles, analysing data available from a thermistor mooring deployed in the lake's deepest basin and determining the extent of deep water ventilation by the density current initiated at Niagara Falls in Quesnel Lake's East Arm.

7.1 Thorpe Scale

Where the water column is unstable, a Thorpe scale can be used to quantify overturn scales in individual profiles. Instabilities can be identified from density profiles by isolating regions where the density inversions occur (Hohmann et al., 1997). The Thorpe Length, named after Steven A. Thorpe who introduced the concept in 1977 (Thorpe, 1977), can be used to estimate the average eddie size in a region of density inversion. The Thorpe Length is the root mean square of the displacements required to reorder a density profile to be monotonically increasing (Thorpe, 1977). Dillon (1982) compared the Thorpe Scale to the Ozmidov scale, a scale for eddie size predicted using the local turbulent energy budget, and found that, in regions away from the surface, they were in good agreement.

Galbraith and Kelley (1996) outline a procedure for identifying overturn size from CTD data using the Thorpe Scale. They address issues of spatial resolution and outline two tests that are used to isolate real overturns due to density inversions from systematic or instrumental error. These tests are the run length test, which sets out a minimum number of reordered points differentiating real overturns from noise, and the water mass test, which differentiates temperature-salinity spikes from real overturns. This method was illustrated with two profiles, one from the Saint Lawrence Estuary in Canada which is actively mixed and highly stratified and one from near Svalbard in Norway which is less actively mixed and is more weakly stratified. The method showed that with CTD data that is able to resolve density difference on the

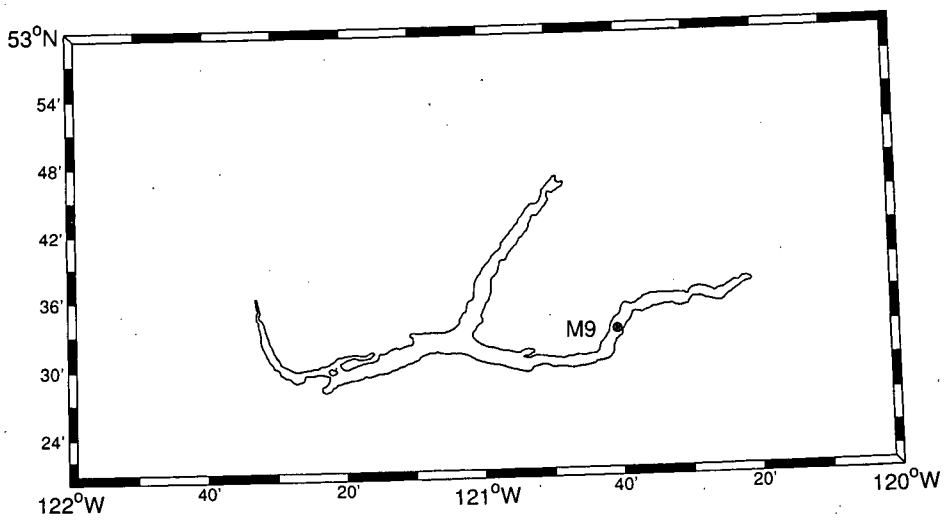

Figure 35: Map showing location of Mooring 9

order of 10^{-3}kg/m^3, overturns thinner than 2m cannot be detected if N 0.003s^{-1} (i.e. weakly stratified). Stansfield et al. (2001) applied the Galbraith and Kelley (1996) method to CTD profiles from the Juan de Fuca Strait which were already reordered and profiles with random noise added to them to evaluate if this method would reject false overturns. Stansfield et al. (2001) concluded that Galbraith and Kelley's method is robust. This method should be applied to Quesnel Lake CTD data to assess if it can be used to identify overturns in Quesnel Lake's weakly stratified water.

7.2 M9 Thermistor Chain

A thermistor chain, called M9, was deployed in the East Arm (see Fig. 35) on September 24th, 2003. Five Brancker TR-1000s and 4 Vemco thermistors were attached to a kevlar line starting from the bottom and set to take temperature readings every hour over the winter months. Table 6 outlines the structure of the mooring. Note distances are measured from the bottom.

The year-long time series of the thermal structure in Quesnel Lake's East Arm produced by this data will has not been analysed to date. Its analysis will allow

Table 6: Depths at which thermisors are attached to Mooring 9 in Quesnel Lake's East Arm.

Distance from Bottom
1m
100m
200m
300m
400m
425m
450m
480m
500m

one to answer questions of whether or not the deep water renewal is an episodic or continual process. Also, presumably the deep water temperature doesn't change significantly throughout the year and data from this mooring will allow us to verify this hypothesis. If the ventilation is indeed episodic, future field work could include the deployment of two thermistor chains in the East Arm. This will allow one to determine from which direction deep water is being ventilated.

7.3 Further Investigation of Density Currents

Transmissivity data, collected in the summer of 2003, could give insight as to weather the limited transparency of the water in Quesnel Lake's East Arm is due to density plume. Also, unloading of density current water could be investigated with settling experiments using Niagara Creek river water. The Department of Civil Engineering at UBC has recently acquired an autonomous underwater vehicle (AUV) capable of simultaneously measuring in situ conductivity, tempeature, pressure, optical backscatter, chlorophyll A, and water velocity at depths of up to 500m. Further research could include use of this AUV, coupled with CTD profiles to determined the extent of the density current and potentially an Acoustic Doppler Current Profiler to determine the velocity of the density current.

References

Bradshaw, A. and K. Schleicher (1965). The effect of pressure on the electrical conductance of sea water. *Deep-Sea Research 12*, 151–162.

Campbell, I. J. (2001). *Drawing No. CP01247.* Sidney, B.C.: Coast Pilot, Ltd. ph. no. 250-656-2109.

Carmack, E. C. (1979b). Combined influence of inflow and lake temperatures on spring circulation in a riverine lake. *Journal of Physical Oceanography 9*, 422–434.

Chen, C. and F. Millero (1976). The specific volume of seawater at high pressures. *Deep-Sea Research 23*, 595–612.

Chen, C. and F. Millero (1977a). Effect of salt content on the temperature of maximum density and on static stability in lake ontario. *Limnology and Oceanography 22*(11), 158–159.

Chen, C. and F. Millero (1977b). The use and misuse of pure water pvt properties for lake waters. *Nature 266*, 707–708.

Chen, C. and F. Millero (1986). Precise thermodynamic properties for natural waters covering only the limnological range. *Limnology and Oceanography 31*, 657–662.

Dauphinee, T. M. (1980). Introduction to the special issue on the practical salinity scale 1978. *IEEE Journal of Oceanic Engineering OE-5*(1), 1–3.

Dillon, T. M. (1982). Wertical overturns: A comparison of thorpe and ozmidov length scales. *Journal of Geophysical Research 87*(C12), 9601–9613.

Eklund, H. (1963). Fresh water: Temperature of maximum density calculated from compressibility. *Science 142*, 1457–1458.

Eklund, H. (1965). Stability of lakes near the temperature of maximum density. *Science 149*, 632–633.

Ekman, V. W. (1934). Review of das bodenwasser und die gliederung del atlantischen tiefsee by georg wust. *ICES Journal Of Marine Science 9*, 102–104.

Fisher, T. S. R. (2002, April). *Determination of Salinity and Density in a Meromictic Mine Pit Lake.* Ph. D. thesis, Department of Civil Engineering and Department of Earth and Ocean Science, University of British Columbia, Vancouver, B.C.

Fisheries and Oceans Canada (2001). *Fraser River Sockeye Escapement Estimates; Near Final Estimates, BC Interior Area.* Fisheries and Oceans Canada. Data Report.

Foster, T. D. (1995). Abyssal water mass formation of the eastern wilkes land coast of antarctica. *Deep-Sea Research I 42*(4), 501–522.

Galbraith, P. S. and D. E. Kelley (1996). Identifying Overturns in CTD Profiles. *Journal of Atmospheric and Oceanic Technology 13*, 688–702.

Gill, A. E. (1982). *Atmospheric-Ocean Dynamics.* Academic Press.

Grafe, H. et al. (2002). Ultrasonic in situ measurements of density, adiabatic compressibility and stability frequency. *Limnology and Oceanography 47*(4), 1255–1260.

Gray, C. B. J., R. C. Wiegand, and R. A. Kirkland (1979). Data report on the limnology of kootnay lake, british columbia. conductivity temperature salinity relationships. Technical Report 6, National Water Research Institute, West Vancouver, B.C.

Hill, K. D., T. M. Dauphinee, and D. J. Woods (1986). The extension of the practical salinity scale 1978 to low salinities. *IEEE Journal of Oceanic Engineering OE-11*, 109–111.

Hohmann, R., R. Kipfer, F. Peeters, G. Piepke, , and D. M. Imboden (1997). Processes of deep-water renewal in lake baikal. *Limnology and Oceanography 42*(5), 841–855.

Imboden, D. M. and A. Wuest (1995). Mixing mechanisms in lakes. In A. Lerman, D. Imboden, and J. Gat (Eds.), *Physics and Chemistry of Lakes* (Second ed.). Springer.

Johnson, D. (1989). Conductivity temperature coefficients for the great lakes. Technical report, Environment Canada. Honours Agriculture Semester Five.

Johnson, L. (1964). Temperature regime of deep lakes. *Science 144*, 1336–1337.

Killworth, P. D., E. C. Carmack, P. F. Weiss, and R. Matear (1996). Modeling deep-water renewal in lake baikal. *Limnology and Oceanography 41*(7), 1521–1538.

Lewis, E. L. (1980). The practical salinity scale 1978 and its antecedents. *Journal of Oceanic Engineering OE-5*(1), 3–8.

McDougall, T. J. (1987). Thermobaricity, cabelling and water-mass conversion. *Journal of Geophysical Research 92*, 5448–5464.

McManus, J., R. Collier, J. Dymond, C. G. Wheat, and G. L. Larson (1992). Physical properties of crate lake, oregon: A method for the determination of a conductivity- and temperature-dependent expression for salinity. *Limnology and Oceanography 37*(1), 41–53.

McManus, J., R. Collier, J. Dymond, C. G. Wheat, and G. L. Larson (1996). Spatial and temporal distribution of dissolved oxygen in crater lake, oregon. *Limnology and Oceanography 41*(4), 722–731.

Millard, R. C., W. B. Owens, , and N: P. Fofonoff (1990). On the calculation of the brunt- vaisala frequency. *Deep-Sea Research 37*(1), 167–181.

Millero, F. J. (2000a). Effect of changes in the composition of seawater on the density-salinity relationship. *Deep Sea Research I 47*, 1583–1590.

Millero, F. J. (2000b). The equation of state of lakes. *Aquatic Geochemistry 6*, 1–16.

Millero, F. J., C. T. Chen, A. Bradshaw, and K. Schleicher (1980). A new high pressure equation of state for seawater. *Deep-Sea Research 27A*, 255–264.

Millero, F. J., A. Laferriere, and P. Chetirkin (1977). The partial molal volumes of electrolytes in 0.725m sodium chloride solutions at 25°c. *Journal of Physical Chemisty 81*, 1737–1745.

Morton, K. F. and I. V. Williams (1990). Sockeye salmon oncorhynchus nerka utilization of quesnel lake, british columbia. Technical report, Canadian technical report of fisheries and aquatic sciences.

Peeters, F., G. Piepke, R. Hohmann, and D. M. Imboden (1996). Description of stability and neutrally buoyant transport in freshwater lakes. *Limnology and Oceanography 41*(8), 1711–1724.

Perkin, R. G. and E. L. Lewis (1980). The practical salinity scale 1978: Fitting the data. *IEEE Journal of Oceanic Engineering OE-5*(1), 9–16.

Press, W. H., B. P. Flannery, S. A. Teukolsky, and W. T. Vetterling (1987). *Numerical Recipes, The Art of Scientific Computing.* Cambridge University Press.

Robinson, R. A. and R. H. Stokes (1959). *Electrolyte Solutions* (Second ed.). London: Butterworths.

Royal, L. A. (1966). Problems in rehabilitating the quesnel sockeye run and their possible solution. Technical report, Internation Pacific Salmon Fisheries Commission, New Westminster, B.C., Canada.

Sherstyankin, P. P. and L. N. Kuimova (2002). Thermobaric stability and instability of deep natural waters in lake baikal. *Doklady Earth Sciences 385*(2), 247–251.

Shimaraev, M. N., N. G. Granin, and A. A. Zhdanov (1993). Deep ventilation of lake baikal waters due to spring thermal bars. *Limnology and Oceanography 38*(5), 1068–1072.

Sorensen, J. A. and G. E. Glass (1987). Ion and temperature dependence of electrical conductance for natural waters. *Analytical Chemistry 59*, 1594–1597.

Stansfield, K. L., C. J. R. Garrett, and R. K. Dewey (2001). The probability distribution of the Thorpe displacement within overturns in Juan de Fuca Strait. *Journal of Physical Oceanography 12*, 3421–3434.

Stockner, J. G. and A. C. Costella (1980). The paleolimnology of eight sockeye salmon (Oncorhynchus nerka) nursery lakes in British Columbia, Canada. Technical report, Canadian technical report of fisheries and aquatic sciences.

Strom, K. M. (1945). The temperature of maximum density for fresh waters. *Geofysiske Publikasjoner 16*(8).

Thompson, W. F. (1945). Effect of the obstruction at hell's gate on the sockeye salmon of the fraser river. Technical Report 1, International Pacific Salmon Fisheries Commission.

Thorpe, S. A. (1977). Turbulence and mixing in a scottish loch. *Philisophical Transactions of the Royal Society of London. Series A, Mathematical and Physical Science 286*(1334), 125–181.

UNESCO (1981, 1-5 September 1980). Tenth report of the joint panel on oceanographic tables and standards. In *UNECA technical papers in marine science*, Volume 36, Sidney, BC, Canada.

Vollmer, M. K., R. F. Weiss, R. T. Williams, K. K. Falkner, X. Qiu, E. A. Ralph, and V. V. Romanovsky (2002b). Physical and chemical properties of the waters of saline lakes and their importance for deep-water renewal: Lake issyk-kul, kyrgyzstan. *Geochimica et Cosmochimica Acta 66*(24), 4235–4246.

Weiss, R. F., E. C. Carmack, and V. M. Koropalov (1991). Deep-water renewal and biological production in lake baikal. *Nature 349*, 665–669.

Wuest, A. (1999). Equation of state for arrow reservoir water. In R. Pieters (Ed.), *Arrow Reservoir Limnology and Trophic Status Year 2 (1998/99) Report*, Volume 5. Province of British Columbia Ministry of Environment, Lands and Parks.

Wuest, A., G. Piepke, and J. Halfman (1996). *Limnology, Climatology and Paleoclimatology of the East African Lakes*, Chapter Combined Effects of Dissolved Solids and Temperature on the Density Stratification of Lake Malawi, pp. 183–202. Toronto: Gordon and Breach.

A Polynomial Coefficients

A.1 Limiting Equivalent Conductivity

Coefficients for the third order polynomials for limiting equivalent conductivity for ions in large concentration in Quesnel Lake based on data published in Robinson and Stokes (1959). Where limited data is available (i.e. less that 4 temperatures), a second order polynomial is used and a "-" is used to mark the absense of the forth coefficient.

$$\lambda^{\infty} = A + B \cdot T + C \cdot T^2 + D \cdot T^3 \tag{42}$$

Ion	A	B	C	D
Sodium	26.4118	0.7707	0.0082	-4.5001 x 10-5
Chloride	40.9701	1.2891	0.0054	-1.0670 x 10-5
Magnesium	28.9000	0.6957	0.0107	-
Calcium	31.1911	0.9299	0.0087	-2.8035 x 10-5
Nitrate	40.0000	1.2175	3.7871 x 10-5	6.3940 x 10-5
Sulphate	41.0000	1.4251	0.0054	-
Potassium	40.6780	1.1817	0.0061	-3.1577 x 10-5
Carbonate	36.00	1.3804	-0.001073	-
Bicarbonate	24.63	0.70136	0.0053739	-0.00006485

A.2 Reduction Factor

Coefficients for the third order polynomials for the reduction coefficient for ions in large concentration in Quesnel Lake.

$$f_i = A + B \cdot x + C \cdot x^2 + D \cdot x^3 \tag{43}$$

where $x = \sqrt{concentration}$.

Ion	A	B	C	D
Sodium	0.9999	-0.8248	1.586	-0.8723
Chloride	1.0000	-0.6271	0.6855	-0.2695
Magnesium	1.0008	-2.516	5.8629	-6.3597
Calcium	1.0011	-2.3785	5.4562	-5.6325
Nitrate	0.9991	-0.6579	-0.1461	0.7767
Sulphate	1.0022	-2.0353	3.2068	-2.0426
Potassium	1.0003	-0.674	0.9295	-0.658
Carbonate	1.0202	-2.5638	2.4655	2.8852
Bicarbonate	0.9999	-0.8871	1.2214	-4.2751

B The Carbonate System

The carbonate system, which plays an important role in buffering acids and bases, contains most of the carbon found in natural waters and controls the transport of carbon through air-surface interfaces. Gaseous carbon dioxide in the atmosphere equilibrates with aqueous carbon dioxide in the water and in doing so enters the carbonate system. The carbonate system is represented in the diagram below as a series of equilibria between the various components of the carbonate system.

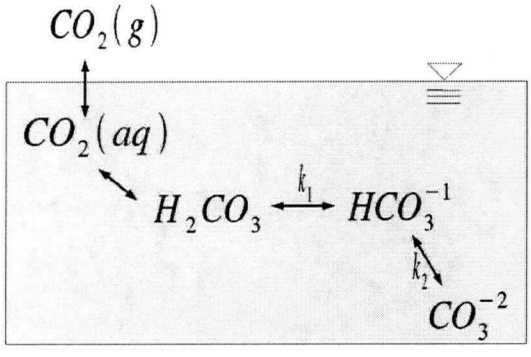

Figure 36: Diagram depicting the equilibrium of components of the Carbonate System.

Although all three components contribute to the density of the water in which they are dissociated, two of three components of the Carbonate System are ionic. For this reason, it is important to find the concentrations of the components and identify their contribution to the conductivity of the water so that the water's density can be determined through conductivity measurements.

The dissociation constant in the reaction in which $[H_2CO_3]$ is ionised, k_1, is defined by:

$$k_1 = \frac{[HCO_3^{-1}][H^{+1}]}{[H_2CO_3]} \tag{44}$$

Similarly, for the ionisation of $[HCO_3^{+1}]$, the dissociation constant, k_2, is defined by:

$$k_2 = \frac{[CO_3^{-2}][H^{+1}]}{[HCO_3^{+1}]} \tag{45}$$

Water is also ionised to a small degree and its dissociation constant, k_w, is defined in a similar way:

$$k_w = \frac{[H^{+1}][OH^{-1}]}{[H_2O]} \tag{46}$$

Equations 44 and 45 can be rearrange to give formulas for finding respectively $[H_2CO_3]$ and $[CO_3^{-2}]$ in terms of $[HCO_3^{-1}]$ as follows:

$$[H_2CO3] = [HCO_3^{-1}] \cdot \frac{10^{-pH}}{10^{-pk_1}} \tag{47}$$

$$[CO_3^{-2}] = [HCO_3^{-1}] \cdot \frac{10^{-pk_2}}{10^{-pH}} \tag{48}$$

These two equations give the concentration of two of the three components of the Carbonate System in terms of pk_1 and pk_2 which are found empirically and pH which can be measured from a water sample. The third, $[HCO_3^{-1}]$, will have to be found indirectly through the measurement of alkalinity. The definition of total alkalinity, TA, is the concentration of all bases that can accept H^+:

$$TA = [HCO_3^{-1}] + 2 \cdot [CO_3^{-2}] + [OH^{-1}] - [H^{+1}] \tag{49}$$

Note that when converting alkalinity concentrations from mg $CaCO_3$/L to equivalents/L, one must remember that both anion and cation have a valence of two and therefore this factor must be included in the conversion.

By substituting Eq. 48 for $[CO_3^{-2}]$ and solving for $[HCO_3^{-1}]$, Eq. 49 becomes:

$$[HCO_3^{-1}] = \frac{TA[H^{+1}] - [OH^{-1}][H^{+1}] + [H^{+1}]^2}{[H^{+1}] + 2 \cdot k_2} \tag{50}$$

Or, by substituting Eq. 46 with $[H_2O] = 1$, Eq. 50 becomes:

$$[HCO_3^{-1}] = \frac{TA[H^{+1}] - k_w + [H^{+1}]^2}{[H^{+1}right] + 2 \cdot k_2} \tag{51}$$

Or,

$$[HCO_3^{-1}] = \frac{TA \cdot 10^{-pH} - 10^{-pk_w} + (10^{-pH})^2}{10^{-pH} + 2 \cdot 10^{-pk_2}} \tag{52}$$

Now, all three parts of Carbonate System are given in terms of pk_1, pk_2, pk_w and pH. The temperature dependence of these variables at low salinities have been found

empirically and are summarised by Millero (2000). The following empirical formulae assume that the water is so dilute that it can be considered fresh water (i.e. $S = 0$):

$$pk_1 = -\log(\exp(290.9097 - \frac{14554.21}{T} - 45.0575 \cdot \ln(T))) \tag{53}$$

$$pk_2 = -\log(\exp(207.6548 - \frac{11843.79}{T} - 33.6485 \cdot \ln(T))) \tag{54}$$

$$pk_w = -\log(\exp(148.9802 - \frac{13847.26}{T} - 23.6521 \cdot \ln(T))) \tag{55}$$

where T is in Kelvin.

With the above equations coupled with measurements of pH and total alkalinity, the temperature dependence of the concentrations of the ionic components of the Carbonate System can be found.

C Matlab Equation of State Toolbox

The Equation of State Toolbox for Matlab has been developed to assist in the delopment of equations of state with lake water chemistry data. The toolbox produces coefficients for the expression of a lake's temperature factor, f_T, and the constant of proportionality, A, required to produce an equation relating in-situ salinity to CTD parameters. In order to relate salinity to density, the coefficient of haline contraction must be determined by the procedure described in Section 3.4 of this text.

The .m files printed below require chemistry data files for input that takes the specific form of chemfile=[pH alk Na NH4 K Ca Mg Cl Fl NO3 SO4 C25 Si] where all concentrations are in units of mg/L.

The flow chart in Fig. 37 illustrates the sequence of steps carried out by the toolbox. An initial script would contain the names of the chemistry files and CTD profiles. Here, densitycalc.m is used as an example. densitycalc.m calls relationships.m which in turn calls C25.m. C25.m, which calculates conductivity of the solution over a range of temperatures, calls a series of operations including: carbonates.m (which calculated the concentration of the components of the carbonate system), equivalents.m (which finds charge difference and equivalent concentration of sample), LEC.m (which finds limiting equivalent conductivity (LEC) for ions over the given temperature range), reductioncoeff.m (which finds reduction coefficient for ions over equivalent concentration range) and keff.m (which finds the effective conductivities for each ion). The conductivity over a range of temperatures outputted to relationship.m which then uses it to calculate the coefficients of f_T. salinity.m is called to calculate the total salinity and the ratio between salinity and specific conductivity — required for determining A. The coefficients of f_T and A are outputted to densitycalc.m which then uses the CTD measurements to calculate the in-situ salinity and density profiles.

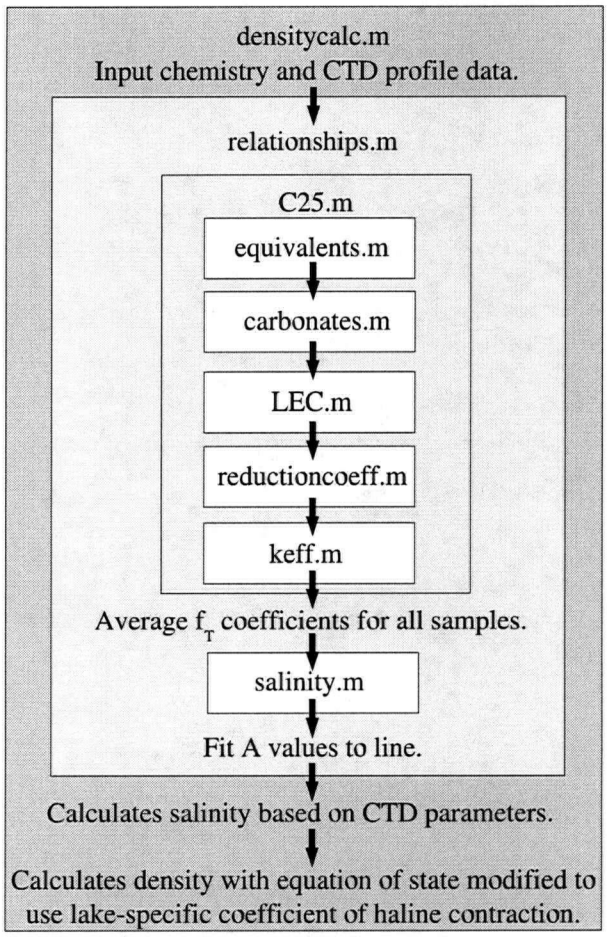

Figure 37: Flowchart of Matlab Equation of State Toolbox.

C.1 densitycalc.m

```
% This script is used to calculate an in-situ density profile
%from CTD profiles and chemistry data.

clear all

%name relevant chemistry data files and CTD files
chemfiles={'filename'};
ctdfiles={'filename'};

binsize=8; %size of bin to smooth quasi-density profile

Zr=0;
%reference depth from with to start calculating quasi density

%find coefficients for finding salinity from CTD data
relationships(chemfiles)
load coeff.mat

for l=1:length(ctdfiles)

    %load ctd data and get data starting at reference depth
    XX=load(ctdfiles{l});
    C=XX(:,1);
    T=XX(:,3);
    P=XX(:,2);

    K=find(P>Zr); %throw out data before reference depth
    P=[Zr; P(K)];
    C=[C(K(1));C(K)];
    T=[T(K(1));T(K)];

    [PP,I]=sort(P); %sort data so that pressure is increasing
    CC=C(I);
```

```
    TT=T(I);

    for i=1:length(P)-1
    %pick out indices with non-reoccuring pressures
        p(i)=PP(i+1)-PP(i);
    end
    PI=find(p~=0);

    new_P=PP(PI); %pick out data with non-reoccuring pressures
    new_C=CC(PI);
    new_T=TT(PI);

    %calculate salinity
    for j=1:length(new_P)
        g=(10^(-5))*(1.856-0.05601*new_T(j)+0.0007*new_T(j)^(2));
%to get fp from fit+T
        fp=1+g*new_P(j);
        S(j)=A*new_C(j)/((ft4+ft3*new_T(j)+ft2*new_T(j)^(2)+ft1...
   *new_T(j)^(3))*(fp));
    end
    S=S';
    SS=S/1000;  %convert to rhocm units

    %calculate in-situ desnity from EOS$_{QL}$
    for j=1:length(new_P)
        rhoQL(j)=rhocm_Quesnel(SS(j),new_T(j),new_P(j));
    end
    rhoQL=rhoQL*1000;

end
```

C.2 relationships.m

```
%RELATIONSHIPS Develop lake-specific relationships.
%
%   [ ]=relationships(chemfiles)
```

```
%
%   Develops lake specific relationships for C25=C25(C,T,P)
%   and determines a value for the empirical constant A using
%   chemfiles with format of filename=[pH alk Na NH4 K Ca...
%    Mg Cl Fl NO3 SO4 C25 Si].
%
%
%   Function called by densitycalc.m.
%
%   Input: name of variable containing chemistry file names.
%   Creates .mat file which contains A and ft coefficients.
%   Saves calculated coefficients as coeff.mat
%
%   Author: Christina James, 2004.

function [ ]=relationships(chemfiles)

% Calculates C25 and makes polynomial fit for temperature factor

a=zeros(size(chemfiles)); %vector - measured specific conductance
b=zeros(size(chemfiles)); %vector - calculated specific conductance
c=zeros(length(chemfiles),4); %matrix for coefficients of ft

for i=1:length(chemfiles)
    [C25exp,C25calc,ftfit]=C25(chemfiles{i});
    a(i)=a(i)+C25exp;
    b(i)=b(i)+C25calc;
    c(i,:)=ftfit;
end

ft1=mean(c(:,1));
ft2=mean(c(:,2));
ft3=mean(c(:,3));
ft4=mean(c(:,4));

d=zeros(size(chemfiles)); %vector of salinity
```

```
e=zeros(size(chemfiles)); %vector of A

for i=1:length(chemfiles)
    [S,A]=salinity(chemfiles{i});
    d(i)=d(i)+S;
    e(i)=e(i)+A;
end

% to make salinity-specific conductivity line go
% through (0,0)
b=[0 b'];
d=[0 d'];

%fit data to find A
[fitA]=polyfit(b,d,1);
Afit=polyval(fitA,b);

% save coefficients calculated in this function as
% a .mat file
A=fitA(1);
save coeff A ft1 ft2 ft3 ft4
```

C.3 C25.m

```
%C25 Find relationship for specific conductance in term of C,T,P.
%
%   [C25exp,C25calc,ftfit]=C25(fname)
%
%   Finds relationship between specific conductance and parameters
%   measured by a CTD (i.e. conductivity, temperature and pressure)
%   over the temperature range of 0 to 25 degC.
%
%   Called by relationships.m
%
%   Inputs: filename (pH alk Na NH4 K Ca Mg Cl Fl NO3 SO4 C25 Si)
%   Outputs: C25 calc, C25 exp, and ftfit
```

```
%
%   Author:  Christina James, 2004.

function [C25exp,C25calc,ftfit]=C25(fname)

% load and declare variables
X=load(fname);
t=0:25;  % temperature range of interest: 0 to 25 oC unless
         % otherwise specified
X(find(isnan(X)))=0; %sets nan=0
C25exp=X(13); % sample's measured specific conductance

% for Na, NH4, K, Ca, Mg, Cl, Fl, NO3, SO4, HCO3, CO3
mmass=[22.99 18.0 39.1 40.08 24.31 35.45 19.0 62.0 96.0 61.01 60.01];
charge=[1 1 1 2 2 2 1 1 1 2 1 2];

%finds the concentration of ionic components of carbonate system
[H2CO3,HCO3,CO3]=carbonates(t,X(1),X(2));

% find molarity of each ion (besides HCO3 and CO3) from measured
% concentrations
for i=3:11
    molarity(i-2)=X(i)/mmass(i-2);
end

% finds charge difference and equivalent concentration of sample
[diff,equivConc]=equivalents(molarity,charge,HCO3,CO3);

% finds limiting equivalent conductivity (LEC) for ions over
% T range
[l]=LEC(t);

% finds reduction coefficient for ions over equivalent
% concentration range
[f]=reductioncoeff(equivConc,t);
```

```
% finds the effective conductivities for each ion from LEC,
% fi and concentration
[k]=keff(molarity,charge,l,f,HCO3,CO3,t);

%finds conductivity of sample over range of temperatures
for i=1:length(t)
    Ksample(i)=k(i,1)+k(i,2)+k(i,3)+k(i,4)+k(i,5)+k(i,6)+k(i,7)+...
       k(i,8)+k(i,9)+k(i,10)+k(i,11);
end

%calculated specific conductance for comparison with measured
C25calc=Ksample(26);

%find ratio of CT/C25 (i.e. fT for C25=f(T,C,P) relationship)
for i=1:length(t)
    ft(i)=Ksample(i)/Ksample(26);
end

% fit this data for fT to a polynomial and plot
[ftfit,s]=polyfit(t,ft,3);
```

C.4 carbonates.m

```
%CARBONATES Calculate concentration of components of carbonate system.
%
%   [H2CO3,HCO3,CO3]=carbonates(t,pH,alk)
%
%   Using equations for pK1, pK2, and pKw from Millero 1995.
%   Equation for calculating concentration of HCO3 is derived on
%   definition of alkalinity, equation for calculating CO3 derived
%   from definition of equilibrium constant.
%
%   A function called by C25.m.
%
%   Input: temperature, pH and alkalinity
%   Output: concentration of H2CO3, HCO3 and CO3 in mmol/L
```

```
%
%   Author:  Christina James, 2004.

function [H2CO3,HCO3,CO3]=carbonates(t,pH,alk)

alk=alk*2/100.078; % sample's alkalinity in mmol/L available for
                   % accepting protons (charge of 2)

%finding the constants of dissociation
for i=1:length(t)
    pK1(i)=6320.81/(t(i)+273.15)-126.3405+19.568*log(t(i)+273.15);
    pK2(i)=5143.69/(t(i)+273.15)-90.1833+14.613*log(t(i)+273.15);
    pKw(i)=-log10(exp(148.9802-13847.26/(t(i)+273.15)-23.6521*...
          log(t(i)+273.15)));
end

%finding the concentration of ionic constituents
for j=1:length(t)
    HCO3(j)=(10^(-pH)*alk/1000-10^(-pKw(j))+(10^(-pH))^2)*...
       1000/(10^(-pH)+2*10^(-pK2(j)));
    CO3(j)=HCO3(j)*10^(-pK2(j))/10^(-pH);
    H2CO3(j)=HCO3(j)*10^(-pH)/10^(-pK1(j));
end

H2CO3=H2CO3';
HCO3=HCO3';
CO3=CO3';
```

C.5 equivalents.m

```
%EQUIVALENTS Calculate the equivalent concentration of a sample.
%
%   [diff,equivConc]=equivalents(molarity,charge,HCO3,CO3)
%
%   A function called by C25.m.
%
```

```
%   Inputs: molarity, charge, concentration of HCO3, CO3.
%   Outputs: charge difference on ions, and equivalent concentration
%   of sample.
%
%   Author:Christina James, 2004.

function [diff,equivConc]=equivalents(molarity,charge,HCO3,CO3)

%find sum of positive charges
for i=1:5;
    P(i)=[molarity(i)*charge(i)];
end
pos=sum(P);
%find sum of negative charges
for i=6:10;
    N(i)=[molarity(i)*charge(i)];
end
neg=sum(N)+HCO3(1)+2*CO3(1);
%finds difference between positive and negative charges
diff=pos-neg;
%converts from meq/L to eq/L and find sqrt of equiv concentration
aveCharge=(pos+neg)*0.001/2;
equivConc=sqrt(aveCharge);
```

C.6 LEC.m

```
%LEC Find limiting equivalent conductivity over a range of
%   temperatures.
%
%   [l]=LEC(t)
%
%   Limiting equivalent conductivity calulated over a temperature
%   range appropriate to the lake in question (i.e. T=0 to T=25
%   deg C).  Uses 3rd order polynomial fits based on published
%   data (Robinson, 1959); 2nd order polynomial where limited data
%   available (i.e. less than 4 temperatures).
```

```
%
%   A function called by C25.m.
%
%   Input: temperature vector
%   Output: an n x m matrix where n is the number of ions in the
%   sample and m is the length of the temperature vector.
%
%   Author:  Christina James, 2004.

function [l]=LEC(t)

for i=1:length(t)

lNa(i)=26.4118+0.7707*t(i)+0.0082*t(i)^2-0.000045001*t(i)^3;
lNH4(i)=40.2+1.2976*t(i)-0.001437*(i)^2+0.000113*(i)^3;
lK(i)=40.678+1.1817*t(i)+0.0061*t(i)^2+0.000031577*t(i)^3;
lCa(i)=31.1911+0.9299*t(i)+0.0087*t(i)^2-0.000028035*t(i)^3;
lMg(i)=28.9+0.6957*t(i)+0.0107*t(i)^2;

lCl(i)=40.9701+1.2891*t(i)+0.0054*t(i)^2-0.00001067*t(i)^3;
lNO3(i)=40+1.2175*t(i)-0.000037871*t(i)^2+0.00006394*t(i)^3;
lSO4(i)=41+1.4251*t(i)+0.0054*t(i)^2;
lHCO3(i)=24.63+0.70136*t(i)+0.0053739*t(i)^2-0.00006485*t(i)^3;
lCO3(i)=36+1.3804*t(i)-0.001073*t(i)^2+0*t(i)^3;

end

l=[lNa' lNH4' lK' lCa' lMg' lCl' lNO3' lSO4' lHCO3' lCO3'];
```

C.7 reductioncoeff.m

```
%REDUCTIONCOEFF Calculates the reduction coefficient as a
%   function of equivalent concentration.
%
%   [f]=reductioncoeff(equivConc,t)
%
```

```
%   Uses polynomial fits to published data (Robinson, 1959; Dean,
%   1979) to give reduction coefficient as a function of sqrt of
%   equivalent concentration of sample.
%
%   A function called by C25.m.
%
%   Input: equivlent concentration (produced by equivalents.m),
%   temp vector.
%   Output: m x n matrix of reduction coefficients where m is the
%   number of ions and n is the length of the temperature vector.
%
%   Author:Christina James, 2004.

function [f]=reductioncoeff(equivConc,t)

for i=1:length(t)

fNa(i)=0.9999-0.8248*equivConc+1.586*equivConc^2-0.8723*equivConc^3;
fNH4(i)=1-0.674*equivConc+0.6658*equivConc^2-0.3118*equivConc^3;
fK(i)=1.0003-0.674*equivConc+0.9295*equivConc^2-0.658*equivConc^3;
fCa(i)=1.0011-2.3785*equivConc+5.4562*equivConc^2-5.6325*equivConc^3;
fMg(i)=1.0008-2.516*equivConc+5.8629*equivConc^2-6.3597*equivConc^3;

fCl(i)=1-0.6271*equivConc+0.6855*equivConc^2-0.2695*equivConc^3;
fNO3(i)=0.9991-0.6579*equivConc-0.1461*equivConc^2+0.7767*equivConc^3;
fSO4(i)=1.0022-2.0353*equivConc+3.2068*equivConc^2-2.0426*equivConc^3;
fHCO3(i)=0.9999-0.8871*equivConc+1.2214*equivConc^2-4.2751*equivConc^3;
fCO3(i)=1.0202-2.5638*equivConc+2.4655*equivConc^2+2.8852*equivConc^3;

end

f=[fNa' fNH4' fK' fCa' fMg' fCl' fNO3' fSO4' fHCO3' fCO3'];
```

C.8 keff.m

```
%EQUIVALENTS Calculate the equivalent concentration of a sample.
%
%   [diff,equivConc]=equivalents(molarity,charge,HCO3,CO3)
%
%   A function called by C25.m.
%
%   Inputs: molarity, charge, concentration of HCO3, CO3.
%   Outputs: charge difference on ions, and equivalent
%   concentration of sample.
%
%   Author:Christina James, 2004.


function [diff,equivConc]=equivalents(molarity,charge,HCO3,CO3)

%find sum of positive charges
for i=1:5;
    P(i)=[molarity(i)*charge(i)];
end
pos=sum(P);

%find sum of negative charges
for i=6:10;
    N(i)=[molarity(i)*charge(i)];
end
neg=sum(N)+HCO3(1)+2*CO3(1);

%finds difference between positive and negative charges
diff=pos-neg;

%converts from meq/L to eq/L and find sqrt of equiv
%concentration
aveCharge=(pos+neg)*0.001/2;
equivConc=sqrt(aveCharge);
```

C.9 salinity.m

```
%SALINITY Calculates salinity of samples.
%
%   [S,A]=salnity(fname)
%
%   Calculates salinity by summing concentrations of all dissolved
%   componentes (ionic and non-ionic).  Also determines the ratio (A)
%   between salinity and measured specific conductance.
%
%   Called by relationships.m.
%
%   Input: filename (ie.chemistry file entered in EOS_CJ.m)
%   Output: total salinity in mg/L and A in mg*cm/(L*microS).
%
%   Author: Christina James, 2004.

function [S,A]=salinity(fname)

X=load(fname);

t=25; %calculate salinity at a reference temperature

[H2CO3,HCO3,CO3]=carbonates(t,X(1),X(2));
%calcuates components of carbonate system
H2CO3=H2CO3*62.01;, HCO3=HCO3*61.01;, CO3=CO3*60.01;
%convert back to mg/L

x=[X(3) X(4) X(5) X(6) X(7) X(8) X(9) X(10) X(11) ...
   X(13) H2CO3 HCO3 CO3];
S=sum(x); %sum of all components dissolved in sample

A=S/X(12);
```